RhoA–ROCK and p38MAPK-MSK1 mediate vitamin D effects on gene expression, phenotype, and Wnt pathway in colon cancer cells

Paloma Ordóñez-Morán,[1] María Jesús Larriba,[1] Héctor G. Pálmer,[1] Ruth A. Valero,[2] Antonio Barbáchano,[1] Mireia Duñach,[3] Antonio García de Herreros,[4] Carlos Villalobos,[2] María Teresa Berciano,[5] Miguel Lafarga,[5] and Alberto Muñoz[1]

[1]Instituto de Investigaciones Biomédicas "Alberto Sols," Consejo Superior de Investigaciones Científicas-Universidad Autónoma de Madrid, E-28029 Madrid, Spain
[2]Instituto de Biología y Genética Molecular, Consejo Superior de Investigaciones Científicas-Universidad de Valladolid, E-47003 Valladolid, Spain
[3]Facultad de Medicina, Universidad Autónoma de Barcelona, E-08193 Bellaterra, Spain
[4]Unitat de Biologia Cellular i Molecular, Institut Municipal d'Investigació Mèdica, Universitat Pompeu Fabra, E-08003 Barcelona, Spain
[5]Departamento de Anatomía y Biología Celular, Unidad de Biomedicina, Consejo Superior de Investigaciones Científicas-Universidad de Cantabria, E-39011 Santander, Spain

The active vitamin D metabolite 1,25-dihydroxyvitamin D_3 ($1,25(OH)_2D_3$) inhibits proliferation and promotes differentiation of colon cancer cells through the activation of vitamin D receptor (VDR), a transcription factor of the nuclear receptor superfamily. Additionally, $1,25(OH)_2D_3$ has several nongenomic effects of uncertain relevance. We show that $1,25(OH)_2D_3$ induces a transcription-independent Ca^{2+} influx and activation of RhoA–Rho-associated coiled kinase (ROCK). This requires VDR and is followed by activation of the p38 mitogen-activated protein kinase (p38MAPK) and mitogen- and stress-activated kinase 1 (MSK1). As shown by the use of chemical inhibitors, dominant-negative mutants and small interfering RNA, RhoA–ROCK, and p38MAPK-MSK1 activation is necessary for the induction of *CDH1*/E-cadherin, *CYP24*, and other genes and of an adhesive phenotype by $1,25(OH)_2D_3$. RhoA–ROCK and MSK1 are also required for the inhibition of Wnt–β-catenin pathway and cell proliferation. Thus, the action of $1,25(OH)_2D_3$ on colon carcinoma cells depends on the dual action of VDR as a transcription factor and a nongenomic activator of RhoA–ROCK and p38MAPK-MSK1.

Introduction

The active vitamin D metabolite 1,25-dihydroxyvitamin D_3 ($1,25(OH)_2D_3$) is a pleiotropic hormone with broad regulatory effects on the proliferation, differentiation, and survival of many cell types (Ordóñez-Morán et al., 2005; Campbell and Adorini, 2006). On the basis of extensive epidemiological and preclinical evidence (Grant and Garland, 2004; Giovannucci et al., 2006; Wu et al., 2007), $1,25(OH)_2D_3$ and several less calcemic derivatives are currently under clinical study alone or in combination as potential agents against colorectal cancer and other neoplasias (Schwartz et al., 2005; Agoston et al., 2006; Deeb et al., 2007). $1,25(OH)_2D_3$ inhibits the proliferation and promotes the differentiation to a normal adhesive epithelial phenotype of human colon cancer cells through the transcriptional activation of *CDH1* gene encoding E-cadherin and the antagonism of the Wnt–β-catenin signaling pathway (Pálmer et al., 2001), which is aberrantly activated in >80% of human colorectal cancers. E-cadherin is the critical component of the adherens junctions, the intercellular structure needed for the correct formation of compact epithelial layers (Pérez-Moreno et al., 2003). Loss of E-cadherin expression is a requisite for cell deadhesion and migration during the epithelial to mesenchymal

Correspondence to amunoz@iib.uam.es

H.G. Pálmer's present address is Institut de Recerca Vall d'Hebron, E-08035 Barcelona, Spain.

Abbreviations used in this paper: $1,25(OH)_2D_3$, 1,25-dihydroxyvitamin D_3; ATF1, activating transcription factor 1; CREB, cAMP response element-binding protein; DKK-1, dickkopf-1; DRB, 5,6-dichlorobenzimidazole riboside; ERK, extracellular signal-regulated kinase; MSK1, mitogen- and stress-activated kinase 1; *OCN*, *osteocalcin*; *OPN*, *osteopontin*; qRT-PCR, quantitative RT-PCR; PRK2, protein-related kinase 2; ROCK, Rho-associated coiled kinase; shRNA, small hairpin RNA; TCF, T cell factor; VDR, vitamin D receptor; WB, Western blotting.

The online version of this article contains supplemental material.

The Rockefeller University Press $30.00
J. Cell Biol. Vol. 183 No. 4 697–710
www.jcb.org/cgi/doi/10.1083/jcb.200803020

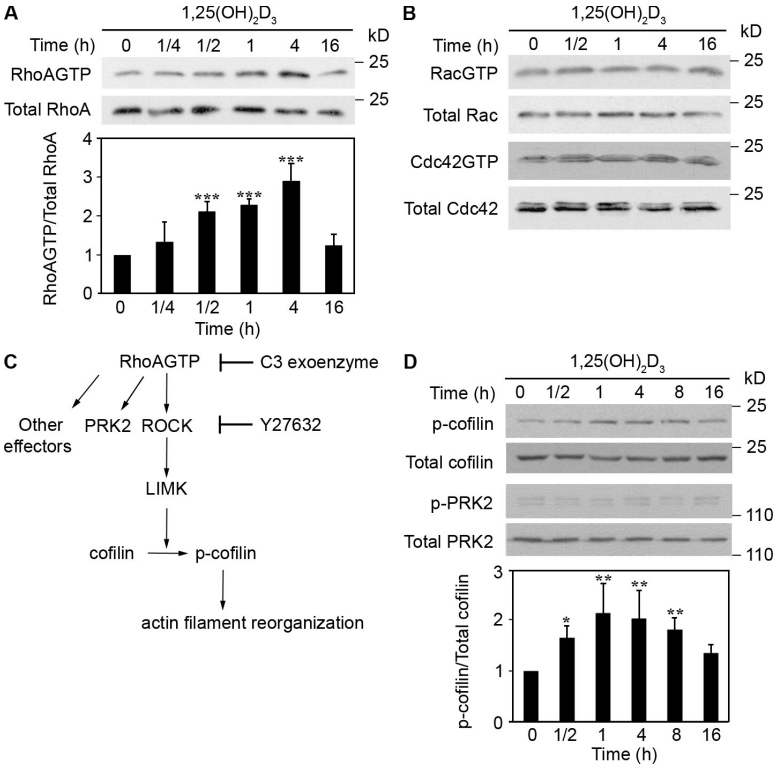

Figure 1. **$1,25(OH)_2D_3$ activates the RhoA–ROCK pathway.** (A) SW480-ADH cells were treated with $1,25(OH)_2D_3$ for the indicated times and RhoA activity was determined by GST pulldown. Normalized RhoAGTP levels are expressed as the mean ± SD (n = 3). (B) $1,25(OH)_2D_3$ does not modulate Rac or Cdc42. Levels of active Rac (RacGTP) and Cdc42 (Cdc42GTP) were determined by GST pulldown in cells after $1,25(OH)_2D_3$ addition. (C) Scheme of biochemical routes triggered by RhoAGTP and sites of inhibition by C3 exoenzyme and Y27632. (D) Cells were treated with $1,25(OH)_2D_3$ for the indicated times and the level of phosphocofilin (p-cofilin) and phospho-PRK2 (p-PRK2) were determined by WB. Normalized p-cofilin levels are expressed as the mean ± SD (n = 3). *, P < 0.05; **, P < 0.01; ***, P < 0.001.

transition and is common in carcinomas (Takeichi, 1993). Activation of the Wnt–β-catenin pathway by mutation of intracellular components such as *APC*, *AXIN*, or *CTNNB1*/β-catenin genes or epigenetic alteration of Wnt inhibitors such as *DKK-1*, *SFRPs*, or *WIF* is the initial step in colorectal tumorigenesis (van de Wetering et al., 2002; Sancho et al., 2004). The interference of $1,25(OH)_2D_3$ with the Wnt–β-catenin pathway relies on the rapid induction of vitamin D receptor (VDR)–β-catenin complexes that titrate out β-catenin, thus hampering formation of the transcriptional competent β-catenin–T cell factor (TCF) complexes that regulate genes involved in tumorigenesis (Pálmer et al., 2001; Shah et al., 2006). Linked to E-cadherin induction, β-catenin later relocates from the nucleus to the adherens junctions (Pálmer et al., 2001). In contrast, the mechanisms leading to the induction of *CDH1*/E-cadherin and the drastic reorganization of the cytoskeleton by $1,25(OH)_2D_3$ remain unknown.

$1,25(OH)_2D_3$ binds to and activates a member of the superfamily of nuclear receptors, the VDR, which is present in >30 cell types and acts as a ligand-modulated transcription factor regulating gene expression (genomic action). The current model for gene activation by $1,25(OH)_2D_3$-VDR predicts that unliganded VDR bound to regulatory sequences (vitamin D response elements) in target genes represses their transcription by recruiting corepressors and histone deacetylases. $1,25(OH)_2D_3$ induces a conformational change in VDR that results in the replacement of corepressors by coactivators and an increased histone acetylase activity, which decondenses chromatin, thus allowing gene activation by the basal RNA polymerase II transcription machinery (Sutton and MacDonald, 2003). $1,25(OH)_2D_3$ drastically alters the gene expression profile of many cell types: in human SW480-ADH colon carcinoma cells it regulates >200 genes involved in cell proliferation, differentiation, survival, invasiveness, and metastatic potential and also in basic cell functions (Pálmer et al., 2003). Additionally, rapid, transcription-independent (nongenomic) actions of $1,25(OH)_2D_3$ on cytosolic kinases, phosphatases, phospholipases, or membrane ion channels have been described, although their role and relevance for the anticancer action of $1,25(OH)_2D_3$ and their relation to the genomic effects are poorly understood (Losel et al., 2003; Norman et al., 2004).

Here we demonstrate that transcriptional activation by $1,25(OH)_2D_3$ of E-cadherin and *CYP24*, which is its most responsive target gene that encodes the $1,25(OH)_2D_3$ 24-hydroxylase (Vaisanen et al., 2005), is mediated by a Ca^{2+}-dependent transient activation of the small GTPase RhoA and its immediate effector Rho-associated coiled kinase (ROCK). Thereafter, $1,25(OH)_2D_3$ activates the p38MAPK and its target the mitogen- and stress-activated kinase 1 (MSK1). Activity of these kinases is required for induction of *CDH1*/E-cadherin transcription and the acquisition of an adhesive epithelial phenotype and for the inhibition of β-catenin–TCF transcriptional activity. Our results indicate that the gene regulatory activity of $1,25(OH)_2D_3$ and its antiproliferative and prodifferentiation effects depend on the early, nongenomic increase in cytosolic Ca^{2+} concentration ($[Ca^{2+}]_{cyt}$) and the subsequent activation of RhoA–ROCK and p38MAPK-MSK1.

Results

$1,25(OH)_2D_3$ induces Ca^{2+} influx and activates RhoA

As the Rho family of GTPases are key regulators of cytoskeleton dynamics and cell adhesion and migration (Burridge and

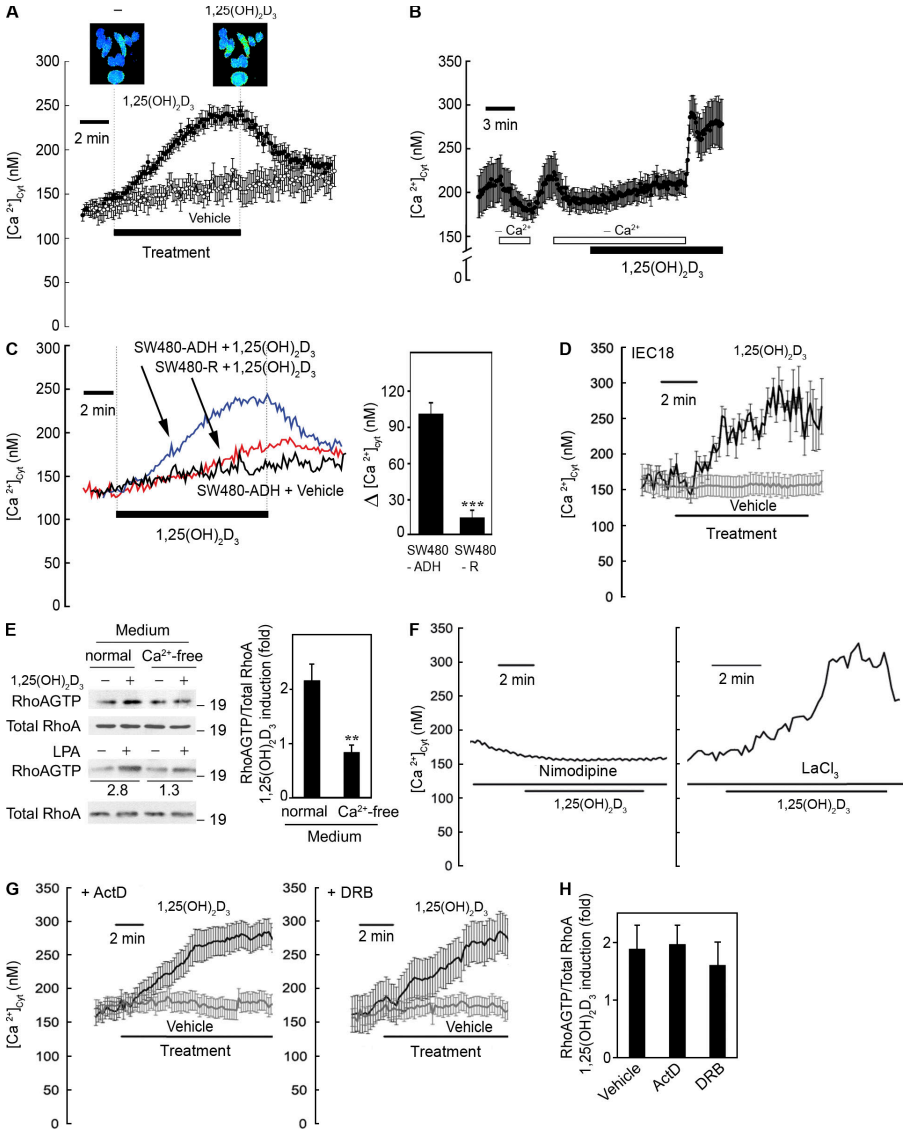

Figure 2. **1,25(OH)$_2$D$_3$ induces Ca^{2+} influx in SW480-ADH cells.** (A) SW480-ADH cells were loaded with fura2/AM, perfused with external medium, and treated with 1,25(OH)$_2$D$_3$ (4×10^{-7} M) or vehicle at the times indicated, and the $[Ca^{2+}]_{cyt}$ was estimated by fluorescence imaging. Records are mean ± SEM of 19–27 cells representative of six independent experiments. Insets show fluorescence images coded in pseudocolor of fura2/AM-loaded SW480-ADH cells before and after stimulation with 1,25(OH)$_2$D$_3$. (B) Cells were incubated in normal or in Ca^{2+}-free medium and treated with 1,25(OH)$_2$D$_3$ as indicated. Data of $[Ca^{2+}]_{cyt}$ are the mean ± SEM of 19 cells representative of three independent experiments. (C) SW480-ADH and SW480-R cells were incubated with 1,25(OH)$_2$D$_3$ or vehicle as indicated. The increase in $[Ca^{2+}]_{cyt}$ (right) corresponds to the maximum detected along the stimulation period for 211 and 169 individual cells studied in six independent experiments for each cell type. The mean increase in untreated cells during a similar period was subtracted. (D) IEC18 cells were loaded with fura2/AM and treated with vehicle or 1,25(OH)$_2$D$_3$ as indicated. Records are mean ± SEM of 33 and 28 cells, respectively, representative of two independent experiments. (E) SW480-ADH cells were incubated with 1,25(OH)$_2$D$_3$, lysophosphatidic acid (LPA), or the corresponding vehicle for 1 h in normal or in Ca^{2+}-free medium. Normalized RhoAGTP levels are expressed as the mean ± SD (n = 3). (F) SW480-ADH cells were incubated with 1 μM nimodipine (left) or 20 μM $LaCl_3$ (right) and then with 1,25(OH)$_2$D$_3$ as indicated. Ca^{2+} measurements are mean ± SEM of 24 cells representative of two independent experiments. (G) Cells were preincubated with 2 μg/ml actinomycin D (ActD; left) or 75 μM DRB (right) for 30 min before 1,25(OH)$_2$D$_3$ treatment. Ca^{2+} measurements are mean ± SEM of 30 cells representative of three independent experiments. (H) Cells were treated with ActD or DRB as in G, and with 1,25(OH)$_2$D$_3$ or vehicle for 1 h. Normalized RhoAGTP levels are expressed as the mean ± SD (n = 3). **, $P < 0.01$; ***, $P < 0.001$.

Wennerberg, 2004), we examined their role in the phenotypic changes induced by 1,25(OH)$_2$D$_3$ in SW480-ADH cells. 1,25(OH)$_2$D$_3$ caused a transient activation of RhoA, as measured by the increase in the level of RhoAGTP, but not of Rac or Cdc42, without affecting the RNA (unpublished data) or protein expression of any of these GTPases (Fig. 1, A and B). Other hormones acting through nuclear receptors such as estrogen, retinoic acid, or dexamethasone had no effect on RhoA activity (unpublished data). 1,25(OH)$_2$D$_3$ transiently increased the phosphorylation of cofilin, a downstream ROCK effector involved in cytoskeleton reorganization (Maekawa et al., 1999), but not of protein-related kinase 2 (PRK2; Fig. 1, C and D).

Next, we explored a possible link between activation of RhoA, which in some systems is Ca^{2+} dependent (Sakurada et al., 2003), and the 1,25(OH)$_2$D$_3$-induced changes in intracellular Ca^{2+} levels reported in several cell types (Losel and Wehling, 2003). The resting $[Ca^{2+}]_{cyt}$ was relatively high in SW480-ADH cells. 1,25(OH)$_2$D$_3$ induced a marked increase in $[Ca^{2+}]_{cyt}$ as registered in individual cells by fluorescence imaging, which was sustained as long as 1,25(OH)$_2$D$_3$ was present (Fig. 2 A). Removal of external Ca^{2+} abolished this increase, whereas its readdition induced a small Ca^{2+} overshoot (Fig. 2 B). This finding indicates that the effect was caused the maintenance of Ca^{2+} entry rather than the transient release of Ca^{2+} from intracellular stores. In SW480-R cells, derived from the same parental line as SW480-ADH but expressing very little VDR (Pálmer et al., 2001), 1,25(OH)$_2$D$_3$ induced a much lower, delayed $[Ca^{2+}]_{cyt}$ rise that was difficult to distinguish from the gradual increase in $[Ca^{2+}]_{cyt}$ in vehicle-treated cells (Fig. 2 C). The slight increase in $[Ca^{2+}]_{cyt}$ in SW480-R cell cultures was caused by only a few cells (Fig. 2 C). Moreover, VDR knockdown by means of small hairpin RNA (shRNA) abolished the increase in $[Ca^{2+}]_{cyt}$ (see Fig. 8 C). These results indicate that VDR mediates Ca^{2+} influx. However, although the presence of small amounts of VDR in caveolae has been postulated in some cell types (Huhtakangas et al., 2004), we did not detect VDR at the plasma membrane by immunofluorescence. Furthermore, incubation with an anti-VDR antibody did not

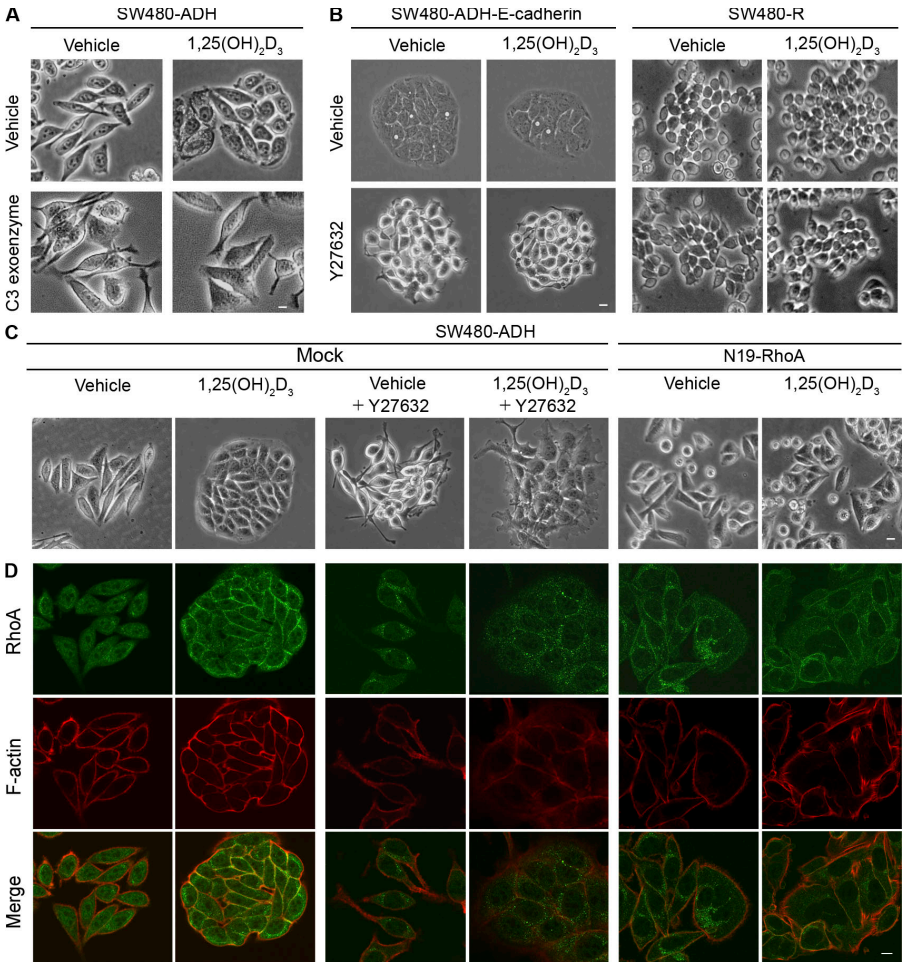

Figure 3. **RhoA–ROCK activation is necessary for the induction of adhesive phenotype by 1,25(OH)$_2$D$_3$.** (A) Phase-contrast microscopy of cells pretreated with 2 µg/ml of C3 exoenzyme for 2 h and incubated with 1,25(OH)$_2$D$_3$ or vehicle for an additional 24 h. (B) Phase-contrast microscopy of both SW480-ADH cells stably expressing exogenous mouse E-cadherin (SW480-ADH-E-cadherin) and SW480-R cells incubated with 1,25(OH)$_2$D$_3$ or vehicle in the presence or absence of 10 µM Y27632 for 48 h. (C) Phase-contrast micrographs of mock cells pretreated for 4 h with 10 µM Y27632 or vehicle and of N19-RhoA cells upon incubation with 1,25(OH)$_2$D$_3$ or vehicle for 48 h. (D) Confocal laser microscopy images of mock and N19-RhoA cells treated as in C. Costaining for the localization of RhoA (green) and F-actin (red). Merged images are also shown. All scanned, phase-contrast, and confocal microscopy images are representative of at least three independent experiments. Bars, 10 µm.

affect the increase in $[Ca^{2+}]_{cyt}$ (unpublished data). Remarkably, 1,25(OH)$_2$D$_3$ also increased $[Ca^{2+}]_{cyt}$ in the nontumoral rat intestine IEC18 cell line (Fig. 2 D). We explored a possible association between the effects of 1,25(OH)$_2$D$_3$ on $[Ca^{2+}]_{cyt}$ and RhoA. Incubation in Ca^{2+}-free medium abolished the activation of RhoA by its reported activator lysophosphatidic acid and also by 1,25(OH)$_2$D$_3$, indicating that Ca^{2+} influx was required for RhoA activation (Fig. 2 E). Nimodipine, an antagonist of the L-type voltage-gated Ca^{2+} channels, but not $LaCl_3$, which blocks store-operated Ca^{2+} channels, prevented the increase of $[Ca^{2+}]_{cyt}$ (Fig. 2 F). Both Ca^{2+} influx and RhoA activation are nongenomic 1,25(OH)$_2$D$_3$ effects, as they were not affected by preincubation with the general transcription inhibitor actinomycin D or the RNA polymerase II inhibitor 5,6-dichlorobenzimidazole riboside (DRB; Fig. 2, G and H; and Fig. S1, available at http://www.jcb.org/cgi/content/full/jcb.200803020/DC1). Although the relative abundance of responsive cells was larger at 1,25(OH)$_2$D$_3$ doses of 4×10^{-7} M than at 10^{-7} M (68 ± 8%, n = 157 cells studied in five independent experiments, vs. 50 ± 12%, n = 101 cells studied in three independent experiments), no differences in the increase of $[Ca^{2+}]_{cyt}$ was found at the individual cell level (compare Fig. 2 [A and C] with Fig. S1). The lack of effect of the glucocorticoid hormone dexamethasone on $[Ca^{2+}]_{cyt}$ supported the specificity of 1,25(OH)$_2$D$_3$ action (Fig. S1).

RhoA–ROCK activation mediates the induction of phenotypic change and E-cadherin expression by 1,25(OH)$_2$D$_3$

To study the role of RhoA activation in 1,25(OH)$_2$D$_3$ activity, we first used the C3 exoenzyme transferase, a Rho inhibitor (Fig. 1 C). C3 exoenzyme altered the morphology of untreated cells and blocked the induction of an adhesive phenotype by 1,25(OH)$_2$D$_3$ (Fig. 3 A). To confirm the involvement of RhoA in 1,25(OH)$_2$D$_3$ activity we generated SW480-ADH cells stably expressing the dominant-negative mutant N19-RhoA (Fig. S2, available at http://www.jcb.org/cgi/content/full/jcb.200803020/DC1). Expression of HA-tagged N19-RhoA did not affect posttranscriptional up-regulation of VDR by its ligand (Wiese et al., 1992; Fig. S2). Likewise, it did not change the predominant nuclear localization of VDR (unpublished data). N19-RhoA cells showed a more rounded, less adherent phenotype than mock-transfected cells (Fig. 3 C) and defects in cytokinesis that lead to polynucleated cells (Glotzer, 2005; Fig. 3 D). The induction of epithelioid islands by 1,25(OH)$_2$D$_3$ was impaired in N19-RhoA cell cultures and it was also reduced by treatment with the ROCK inhibitor Y27632 (Fig. 1 C and Fig. 3 C). Immunofluorescence and confocal microscopy showed that 1,25(OH)$_2$D$_3$ induced the progressive translocation of RhoA from the cytosol to the cell periphery and its colocalization with actin filaments in SW480-ADH cells (Fig. 3 D). Both expression of N19-RhoA and treatment with

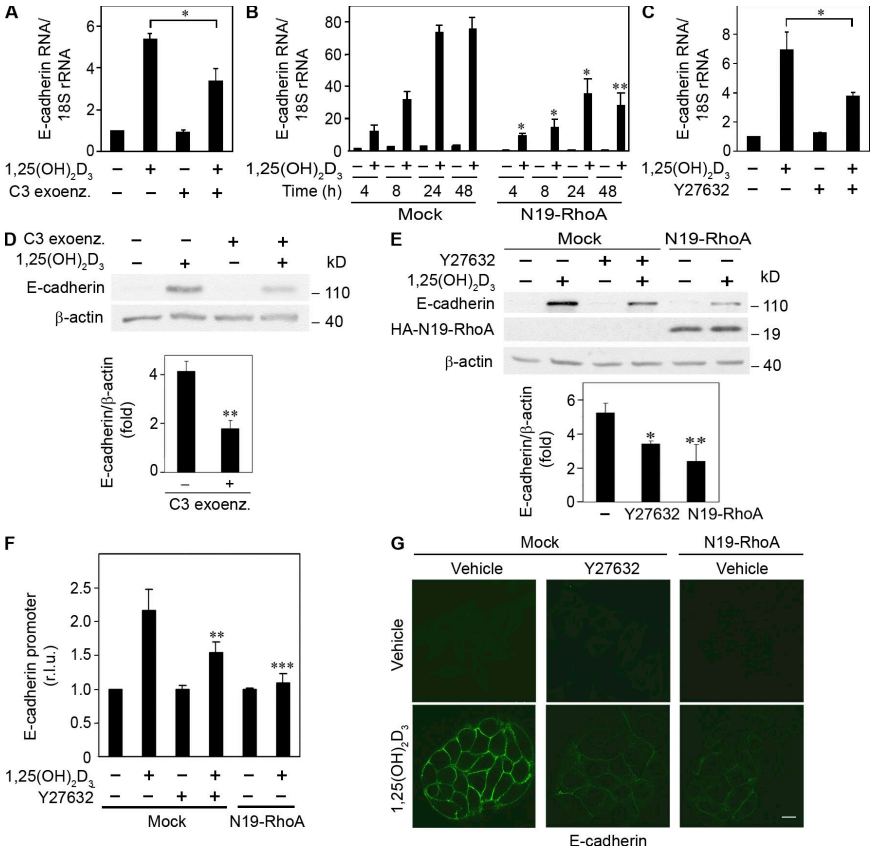

Figure 4. **RhoA–ROCK activation is required for the induction of E-cadherin expression by $1,25(OH)_2D_3$.** (A) SW480-ADH cells were pretreated with 2 µg/ml of C3 exoenzyme or vehicle for 2 h before addition of $1,25(OH)_2D_3$ or vehicle (4 h), and the level of E-cadherin RNA was determined by qRT-PCR. (B) Mock and N19-RhoA cells were treated with $1,25(OH)_2D_3$ as indicated and the level of E-cadherin RNA was determined as in A. (C) SW480-ADH cells were pretreated or not with 10 µM Y27632 for 4 h and then with $1,25(OH)_2D_3$ or vehicle for an additional 4 h, and the level of E-cadherin RNA was determined as in A. The data in A–C are expressed as the mean ± SD (three independent experiments performed in triplicate). (D) SW480-ADH cells were pretreated with C3 exoenzyme (2 h) and then incubated with vehicle or $1,25(OH)_2D_3$ for an additional 20 h, and the level of E-cadherin protein was assessed by WB. Mean ± SD (n = 3). (E) Mock and N19-RhoA cells were incubated with $1,25(OH)_2D_3$ or vehicle (24 h) in the presence or absence of Y27632, and the expression of E-cadherin protein was assessed by WB. Mean ± SD (n = 3). (F) Mock and N19-RhoA cells were transiently transfected with the plasmid encoding a fragment of the human E-cadherin gene promoter. After overnight incubation they were treated with Y27632 (4 h) and then incubated with $1,25(OH)_2D_3$ or vehicle (48 h). Mean ± SD (n = 3); r.l.u., relative luciferase units. (G) Confocal laser microscopy images showing the immunolocalization of E-cadherin in mock cells pretreated or not with Y27632 (4 h) and in N19-RhoA cells incubated with $1,25(OH)_2D_3$ or vehicle (48 h). Bar, 10 µm. *, $P < 0.05$; **, $P < 0.01$; ***, $P < 0.001$.

Y27632 inhibited these $1,25(OH)_2D_3$ effects (Fig. 3 D). Consistent with the role of the RhoA–ROCK pathway in modulating the actin cytoskeleton (Burridge and Wennerberg, 2004) and with the increase by $1,25(OH)_2D_3$ of actin-binding proteins (Pálmer et al., 2003), $1,25(OH)_2D_3$ induced (claudin-7) and redistributed (claudin-7 and occludin) tight junction proteins in a RhoA–ROCK–dependent manner (Fig. S2). Y27632 partially disrupted the strong adhesive phenotype of cells stably expressing an exogenous E-cadherin gene (SW480-ADH-E-cadherin) irrespective of $1,25(OH)_2D_3$ addition, whereas it did not alter the morphology of E-cadherin and VDR-negative SW480-R cells that do not respond to $1,25(OH)_2D_3$ (Fig. 3 B). In contrast, neither the C3 exoenzyme nor Y27632 altered the level of E-cadherin expression in SW480-ADH-E-cadherin cells (Fig. S2). This finding implicates ROCK in E-cadherin–dependent intercellular adhesion. Moreover, Y27632 also altered the adhesive phenotype and impeded $1,25(OH)_2D_3$ action in the more differentiated HT29 colon carcinoma cells, in which RhoA was also activated by $1,25(OH)_2D_3$ as revealed by the increase in phosphocofilin (unpublished data).

Next we examined whether RhoA–ROCK controls E-cadherin induction by $1,25(OH)_2D_3$. The increase of E-cadherin RNA by $1,25(OH)_2D_3$ was reduced by C3 exoenzyme (Fig. 4 A) in N19-RhoA cells (Fig. 4 B) or by addition of Y27632 (Fig. 4 C). The same results were obtained when E-cadherin protein levels were analyzed (Fig. 4, D and E) and on the activation of E-cadherin gene promoter (Fig. 4 F). Collectively, these results indicate that RhoA–ROCK activation is required for the induction of E-cadherin by $1,25(OH)_2D_3$. Accordingly, Y27632 and N19-RhoA inhibited the accumulation of E-cadherin protein at the adherens junctions after $1,25(OH)_2D_3$ treatment of SW480-ADH cells (Fig. 4 G).

RhoA–ROCK activation mediates the gene regulatory action of $1,25(OH)_2D_3$

We also analyzed the role of RhoA–ROCK in the effects of $1,25(OH)_2D_3$ on other targets such as the *CYP24* gene. As for E-cadherin, each of the three agents, C3 exoenzyme, N19-RhoA, and Y27632, decreased the activation of the *CYP24* gene promoter by $1,25(OH)_2D_3$ in SW480-ADH and in SW480-R cells expressing exogenous VDR (Fig. 5, A and B; unpublished data). Accordingly, N19-RhoA and Y27632 also decreased the accumulation of *CYP24* RNA (Fig. 5 C). Moreover, the induction of a series of $1,25(OH)_2D_3$ targets genes such as *osteopontin* (*OPN*), *osteocalcin* (*OCN*), and *CYP3A* at the RNA level and integrin α3, ZO-1, DICKKOPF-1 (DKK-1), $p21^{CIP1}$, and paxillin at the protein level (Pálmer et al., 2001; Ordóñez-Morán et al., 2005; Aguilera et al., 2007) was blunted in N19-RhoA–expressing cells (Fig. 5, D and E). N19-RhoA also inhibited the induction and accumulation of ZO-1 protein at the membrane where it colocalizes with cortical actin filaments (Fig. 5 F). The same result was obtained using Y27632 (unpublished data). Likewise, N19-RhoA and Y27632 inhibited the increase and redistribution of paxillin and the induction of focal contacts and stress fibers by $1,25(OH)_2D_3$ as seen by immunofluorescence (Fig. S3, available at http://www.jcb.org/cgi/content/full/jcb.200803020/DC1). Also in HT29 cells,

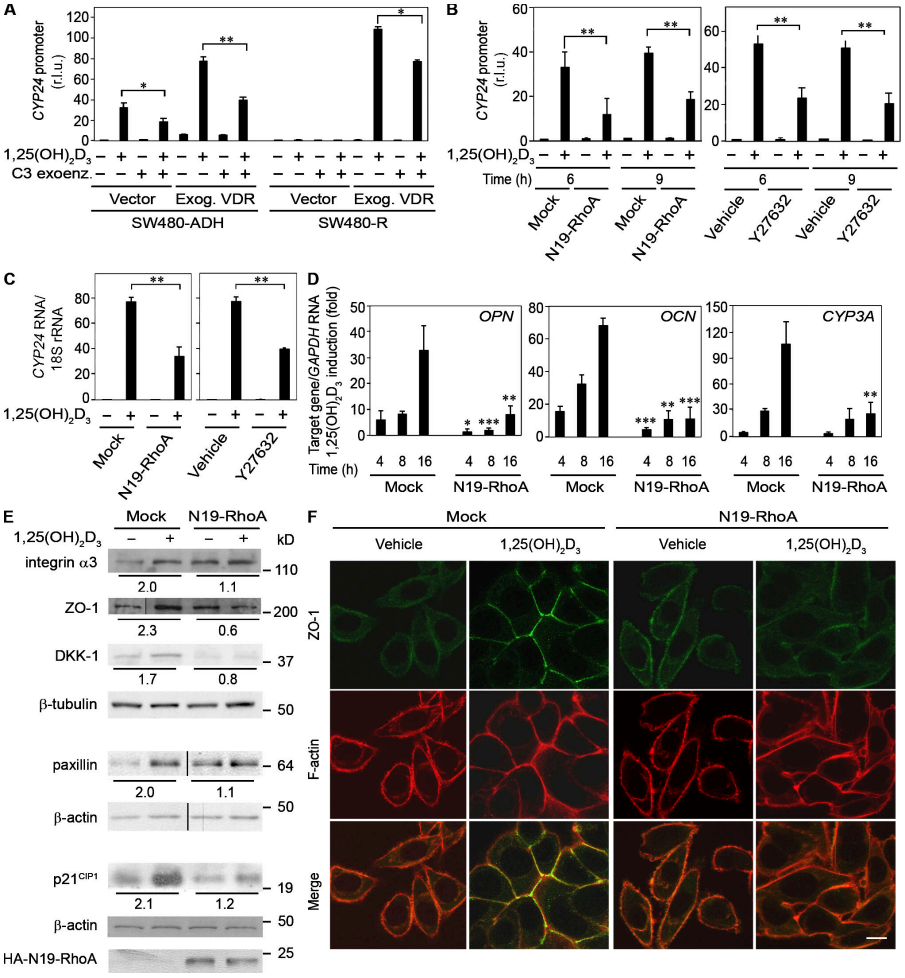

Figure 5. **RhoA–ROCK mediates the induction of *CYP24* and other $1,25(OH)_2D_3$ target genes.** (A) SW480-ADH and -R cells were transiently cotransfected with a plasmid encoding VDR and with a construct containing a fragment of the human *CYP24* promoter-luciferase construct. After overnight incubation the cells were treated with 2 µg/ml of C3 exoenzyme for 2 h as indicated before addition (24 h) of $1,25(OH)_2D_3$ or vehicle. (B) Mock and N19-RhoA cells were transfected with the plasmid encoding a fragment of the human *CYP24* promoter-luciferase construct. After overnight incubation they were treated with $1,25(OH)_2D_3$ or vehicle for 6 or 9 h (left). Mock cells were similarly transfected and then incubated with $1,25(OH)_2D_3$ or vehicle in the presence or absence of 10 µM Y27632 for 4 h (right). (C) Mock or N19-RhoA cells were incubated with $1,25(OH)_2D_3$ or vehicle (4 h) and the level of *CYP24* RNA was determined by qRT-PCR (left). Mock cells were incubated with $1,25(OH)_2D_3$ or vehicle in the presence or absence of 10 µM Y27632 for 4 h and the level of *CYP24* RNA was determined (right). (D) Mock or N19-RhoA SW480-ADH cells were incubated with $1,25(OH)_2D_3$ or vehicle for the indicated times and the expression of *OPN*, *OCN*, and *CYP3A* RNA was determined by qRT-PCR. The data in A–D are expressed as the mean ± SD (three independent experiments performed in triplicate). (E) Mock or N19-RhoA SW480-ADH cells were incubated with $1,25(OH)_2D_3$ or vehicle for 4 ($p21^{CIP1}$) or 48 h (all others), and the expression of integrin α3, ZO-1, DKK-1, paxillin, and $p21^{CIP1}$ proteins were determined by WB. Controls: β-tubulin and -actin. The numbers below tracks represent the fold increase values in $1,25(OH)_2D_3$-treated versus vehicle-treated cells. (F) Confocal laser microscopy images of mock and N19-RhoA cells incubated with $1,25(OH)_2D_3$ or vehicle (48 h) illustrating the localization of ZO-1 (green) and F-actin (red). Bar, 10 µm. *, $P < 0.05$; **, $P < 0.01$; ***, $P < 0.001$.

Y27632 inhibited the increase of *CYP24* RNA, the induction of E-cadherin and vinculin proteins, and the decrease of cyclin D1 by $1,25(OH)_2D_3$ (unpublished data).

RhoA–ROCK activation mediates the antagonism of the Wnt–β-catenin pathway and the inhibition of cell proliferation by $1,25(OH)_2D_3$

$1,25(OH)_2D_3$ induces the relocalization of β-catenin from the nucleus to the plasma membrane adherens junctions, where it binds E-cadherin, thus inhibiting the induction of proliferation and invasion genes by β-catenin–TCF complexes (Pálmer et al., 2001). Coimmunoprecipitation assays revealed that the formation of E-cadherin–β-catenin complexes after $1,25(OH)_2D_3$ addition was decreased in N19-RhoA cells as compared with mock cells (Fig. 6 A). Concordantly, the redistribution of β-catenin from the nucleus and cytosol to the plasma membrane induced by $1,25(OH)_2D_3$ was partially inhibited in N19-RhoA cells or by Y27632 (Fig. 6 B). Likewise, α- and p120-catenins relocated at the plasma membrane after $1,25(OH)_2D_3$ addition and this effect was also diminished in N19-RhoA cells or by Y27632 addition (Fig. 6 B; unpublished data). Moreover, $1,25(OH)_2D_3$ did not repress the transcriptional activity of β-catenin–TCF in N19-RhoA cells, whereas it weakly repressed that activity in Y27632-treated mock cells (Fig. 6 C). These results show that RhoA–ROCK activation is required for the antagonism of the Wnt–β-catenin pathway by $1,25(OH)_2D_3$. In line with the effect of N19RhoA in other systems, N19RhoA cells grew less than mock cells (Fig. 6 D). Additionally, the inhibitory effect of $1,25(OH)_2D_3$ on cell proliferation was lost in N19-RhoA cells (Fig. 6 D).

p38MAPK and MSK1 are activated by $1,25(OH)_2D_3$ and mediate the induction of E-cadherin and *CYP24* gene

As several PKC isoforms respond to changes in Ca^{2+} levels, we studied the effects of PKC inhibitors on $1,25(OH)_2D_3$ action (Fig. S4, available at http://www.jcb.org/cgi/content/full/jcb.200803020/DC1). Ro318220, but not GF109203X, abrogated the increase of E-cadherin protein by $1,25(OH)_2D_3$ (Fig. 7 A). In addition, phosphorylation of PKD, a substrate of PKC, was decreased by GF109203X and Ro318220 but not affected by $1,25(OH)_2D_3$ (Fig. 7 A; unpublished data), thus implicating one or more Ro318220 target kinases other than the PKC family in E-cadherin induction. The candidates were MAPKAP-K1/RSK,

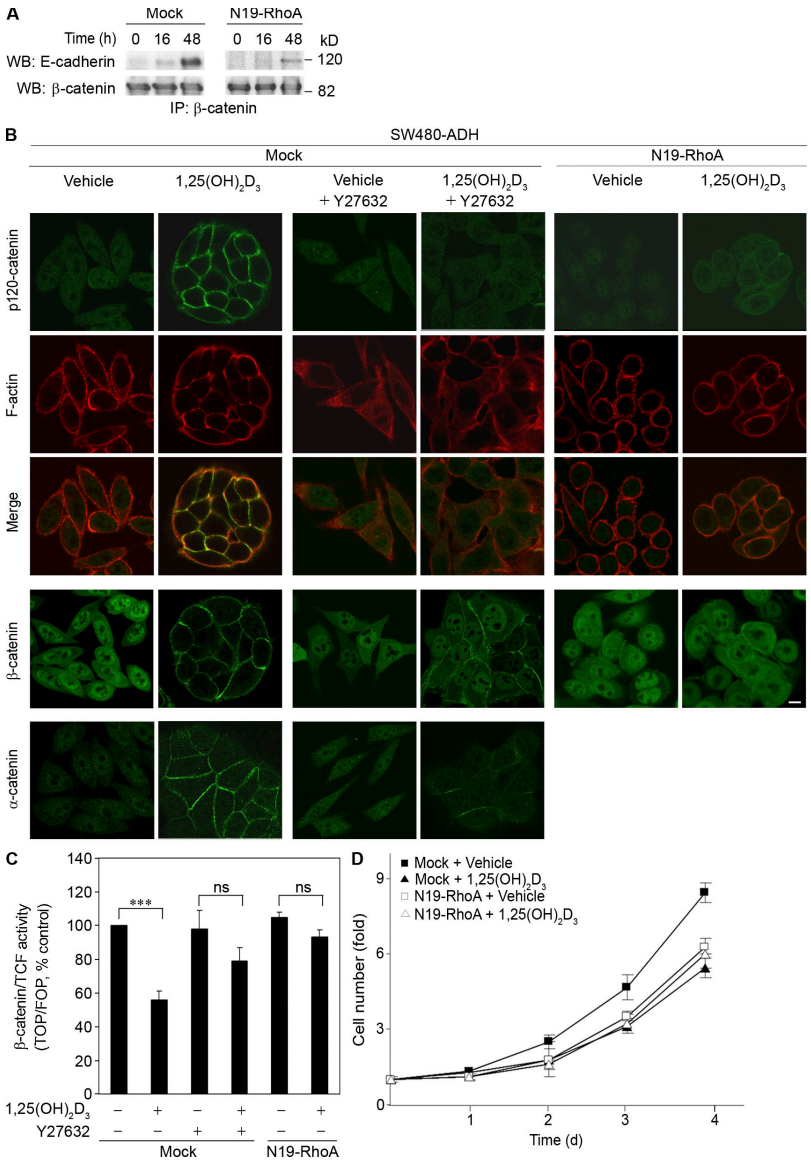

Figure 6. **RhoA–ROCK activation mediates the redistribution of α-, β-, and p120-catenins and the inhibition of β-catenin–TCF transcriptional activity by $1,25(OH)_2D_3$.** (A) Mock and N19-RhoA cells were incubated with $1,25(OH)_2D_3$ for the indicated times and the formation of complexes between E-cadherin and β-catenin was assessed by coimmunoprecipitation (IP). Cell extracts were first immunoprecipitated using an anti–β-catenin antibody and the presence of E-cadherin and β-catenin (as control) in the immunoprecipitates was determined by WB. The IP was repeated four times with similar results. (B) Y27632 and N19-RhoA inhibit the redistribution toward the plasma membrane compartment of α-, β-, and p120-catenins induced by $1,25(OH)_2D_3$. Confocal laser microscopy images of mock (pretreated or not with 10 μM Y27632) and N19-RhoA cells incubated with $1,25(OH)_2D_3$ or vehicle for 48 h. α-, β-, and p120-catenins were stained by immunofluorescence using specific antibodies and F-actin by phalloidin-rhodamine labeling, respectively. The images are representative of at least three independent experiments. Bar, 10 μm. (C) Mock and N19-RhoA SW480-ADH cells were transiently transfected with wild-type (TOP) or mutant (FOP) luciferase-base reporter plasmids for the transcriptional activity of β-catenin–TCF complexes. After overnight incubation, the cells were treated with $1,25(OH)_2D_3$ or vehicle for 48 h in the presence or absence of 10 μM Y27632 and the intracellular luciferase activity was determined. β-catenin–TCF transcriptional activity (TOP/FOP ratio) is expressed as the mean ± SD (n = 3). (D) Mock and N19-RhoA cells were incubated with $1,25(OH)_2D_3$ or vehicle for the indicated times and the number of cells in the cultures was determined. The data represent one out of the four independent experiments performed in triplicate. ***, $P < 0.001$.

MSK1, PRK2, GSK-3β, and S6K1 (Davies et al., 2000). S6K1 was ruled out, as rapamycin, which specifically inhibits its upstream regulator mTOR (Davies et al., 2000), did not prevent the increase of E-cadherin protein by $1,25(OH)_2D_3$ (Fig. S4). PRK2 was neither activated by $1,25(OH)_2D_3$ (Fig. 1 D) nor affected by Ro318220 (Fig. S4). GSK-3β was ruled out as Ro318220 did not increase the level of Snail1 protein, a target of this kinase that accumulates upon GSK-3β blockade by LiCl in SW480-ADH cells (Larriba et al., 2007; unpublished data).

We used additional inhibitors: H89, which inhibits PKA, MSK1, and S6K1 with similar IC_{50} (Davies et al., 2000), decreased E-cadherin induction; and Rp-cAMP, a specific PKA inhibitor (Davies et al., 2000), had no effect (Fig. 7 B). This ruled out PKA and pointed to MSK1. Because MSK1 is activated by either p38MAPK or MKK1–extracellular signal-regulated kinase (ERK; Deak et al., 1998; Dunn et al., 2005), we analyzed the effect of their respective inhibitors, SB203580 and U0126/PD98059. SB203580, but not U0126 or PD98059, decreased the induction of E-cadherin protein (Fig. 7 C; unpublished data), suggesting a role of p38MAPK-MSK1 in mediating $1,25(OH)_2D_3$ action. Furthermore, Ro318220, H89, or SB203580 decreased the phosphorylation of histone H3, an MSK1 substrate (Fig. S4). The link between the activation of p38MAPK and MSK1 was further demonstrated by means of the p38MAPK activator anisomycin, which increased the level of phospho-MSK1 in an SB203580-, H89-, and Ro318220-sensitive manner (Fig. S4).

Consistent with these results, Ro318220, H89, or SB203580, but not GF109203X, Rp-cAMP, or U0126, prevented the induction of E-cadherin RNA (Fig. 7 D). Ro318220 also blocked the activation of the E-cadherin gene promoter (Fig. 7 E). Moreover, similar results were obtained with *CYP24* gene, except that U0126 and Rp-cAMP repressed the accumulation of its RNA (Fig. 7 F) and PD98059 repressed the activation of the promoter by $1,25(OH)_2D_3$ (Fig. S4). Furthermore, in HT29 cells the increase of *CYP24* RNA expression by $1,25(OH)_2D_3$ was inhibited by Ro318220 or SB203580 (unpublished data). These results implicate p38MAPK-MSK1, MKK1-ERK, and PKA in the induction of *CYP24* by $1,25(OH)_2D_3$.

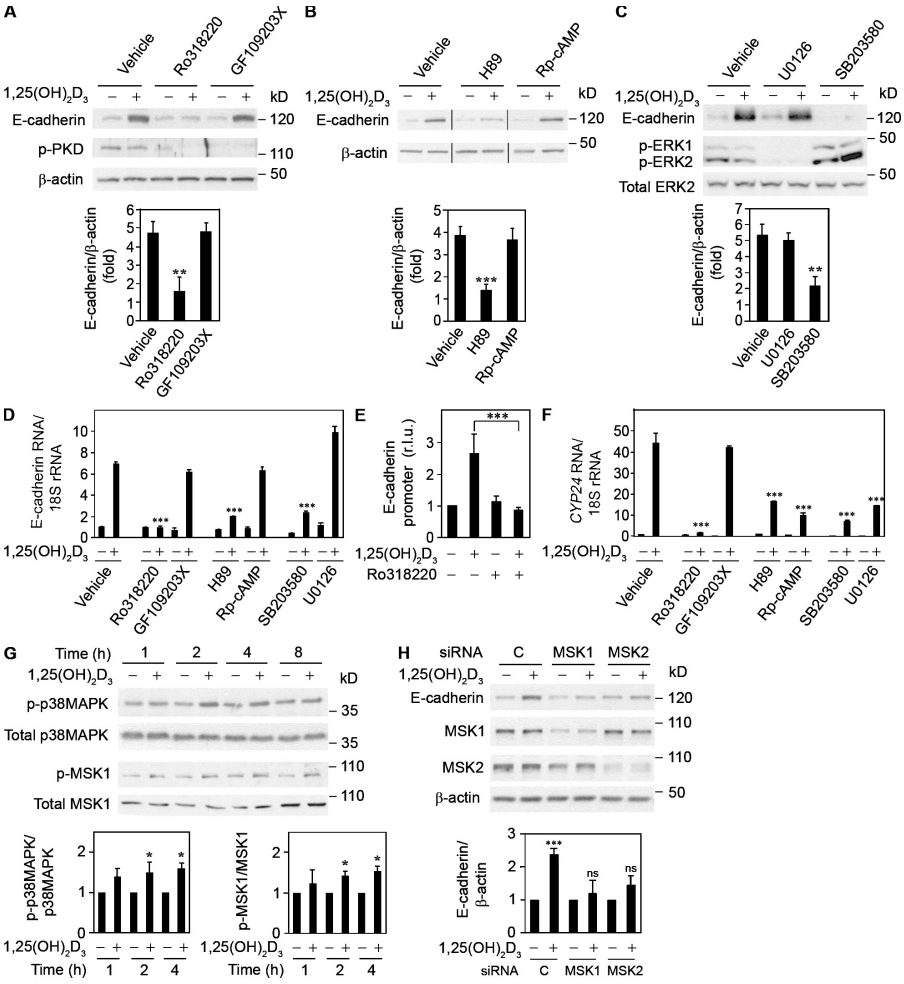

Figure 7. **p38MAPK and MSK1 mediate the induction of E-cadherin and *CYP24* by $1,25(OH)_2D_3$.** (A) SW480-ADH cells were pretreated with either vehicle, 3.5 μM GF109203X, or 2 μM Ro318220 for 2 h before incubation with $1,25(OH)_2D_3$ or vehicle for 20 h, and the level of E-cadherin protein and phosphoprotein kinase D (p-PKD) were determined by WB. Mean ± SD (n = 3). (B) Cells were pretreated with either vehicle, 10 μM H89, or 20 μM Rp-cAMP for 2 h before incubation with $1,25(OH)_2D_3$ for 20 h and E-cadherin protein was determined by WB. Quantification was as in A. (C) Cells were pretreated with either vehicle, 20 μM U0126, or 30 μM SB203580 for 2 h before incubation with $1,25(OH)_2D_3$ or vehicle for 20 h and E-cadherin protein and total and p-ERK1/2 were determined by WB. Quantification was as in A. (D) Cells were incubated (4 h) with $1,25(OH)_2D_3$ or vehicle in the presence or absence of the indicated kinase inhibitor (same doses as in A–C) and E-cadherin RNA was determined by qRT-PCR (three independent experiments performed in triplicate). (E) SW480-ADH cells were transfected with the plasmid encoding a fragment of the human E-cadherin gene promoter. After overnight incubation they were treated (48 h) with $1,25(OH)_2D_3$ or vehicle in the presence or absence of 1 μM Ro318220. Mean ± SD (n = 3). (F) SW480-ADH cells were incubated and treated as in D and the level of *CYP24* RNA was determined and quantificated as in D. (G) Cells were treated with $1,25(OH)_2D_3$ or vehicle and the expression of total and p-p38MAPK and p-MSK1 was determined by WB. Mean ± SD (n = 3). (H) SW480-ADH cells were transfected with MSK1 or MSK2 siRNA oligonucleotides or with scrambled oligos as control (C). 1 d later cells were treated with $1,25(OH)_2D_3$ or vehicle for an additional 6 h. E-cadherin, MSK1, and MSK2 protein levels were determined by WB. Mean ± SD (n = 3). *, P < 0.05; **, P < 0.01; ***, P < 0.001.

We confirmed that $1,25(OH)_2D_3$ increased the level of active, phosphorylated p38MAPK and MSK1 without affecting their total cellular content (Fig. 7 G). Furthermore, $1,25(OH)_2D_3$ increased phosphorylation of the transcription factors cAMP response element-binding protein (CREB) and activating transcription factor 1 (ATF1), which are MSK1 substrates (see Fig. 9 B). Finally, the finding that knockdown of MSK1 or MSK2 by siRNA decreased the induction of E-cadherin is further evidence that these kinases mediate $1,25(OH)_2D_3$ action (Fig. 7 H).

The activation of the signaling pathway by $1,25(OH)_2D_3$ requires VDR and takes place in other tumoral and nontumoral cell lines

To examine the dependence on VDR of the different components of the signaling pathway induced by $1,25(OH)_2D_3$, we knocked down VDR expression in SW480-ADH cells by means of infection with VDR shRNA lentiviruses. Two VDR shRNA (3 and 4) and one control shRNA cell lines were generated. Both VDR shRNA lines showed less intercellular adhesion and more rounded cells than control shRNA cells in both the absence and presence of $1,25(OH)_2D_3$ (Fig. 8 A). We confirmed that VDR shRNA cells expressed less basal and induced VDR protein than control shRNA cells (Fig. 8 B). In addition, VDR shRNA cells had a lower level of E-cadherin protein and showed no induction of *CYP24* promoter in the absence and particularly in the presence of $1,25(OH)_2D_3$ (Fig. 8 B). Likewise, the induction of *CYP24*, *OPN*, *OCN*, and *CYP3A* RNA was blunted in VDR shRNA cells (unpublished data). Remarkably, $1,25(OH)_2D_3$ did not increase $[Ca^{2+}]_{cyt}$ (Fig. 8 C) and did not activate RhoA (Fig. 8 D), p38MAPK (Fig. 8 E), or MSK1 (Fig. 8 F) in VDR shRNA cells. Consistently, it did not increased CREB phosphorylation (Fig. 8 F). Together, these results show that VDR is needed for the induction of the whole signaling pathway by $1,25(OH)_2D_3$.

To know whether p38MAPK-MSK1 mediated the genomic effects of $1,25(OH)_2D_3$ in other cell types we used the SB203580 and Ro318220 inhibitors. First, we checked that both agents inhibited efficiently the phosphorylation of CREB in nontumoral human HaCaT keratinocytes and IMR90 fibroblasts, mouse NIH 3T3 fibroblasts, and rat intestine IEC18 cells (Fig. S5, available at http://www.jcb.org/cgi/content/full/jcb.200803020/DC1). Next, the activation of *CYP24* promoter by $1,25(OH)_2D_3$ was found to be inhibited by Ro318220 or SB203580 in IEC18 and HaCaT and by Ro318220 and H89 in NIH 3T3 cells (Fig. S5). Finally, Ro318220 inhibited the induction by $1,25(OH)_2D_3$ of

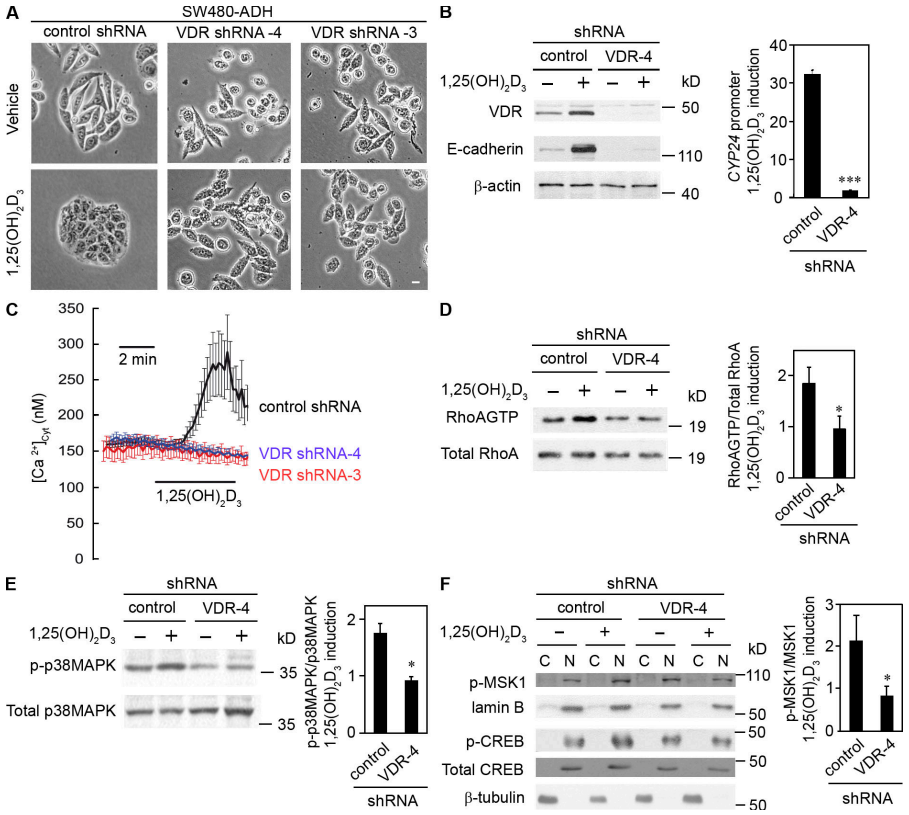

Figure 8. **VDR knockdown abrogates the induction of nongenomic signaling and gene expression by $1,25(OH)_2D_3$.** (A) Phase-contrast images of SW480-ADH cells stably expressing control or VDR shRNA treated with $1,25(OH)_2D_3$ or vehicle for 48 h as indicated. Bar, 10 µm. (B) Expression of VDR and E-cadherin proteins (left) and *CYP24* promoter activity (right) in control and VDR shRNA cells that were treated or not with $1,25(OH)_2D_3$ for 24 h. Protein levels were determined by WB using β-actin as control and *CYP24* promoter activity was analyzed as in legend to Fig. 5. (C) Effect of VDR knockdown on the increase in $[Ca^{2+}]_{cyt}$ induced by $1,25(OH)_2D_3$. The three cell types were loaded with fura2/AM and assessed for responsiveness to $1,25(OH)_2D_3$. Traces are mean ± SEM values of control cells (black) or the two VDR shRNA lines (red and blue traces). Data are representative of at least two independent experiments for each cell line. (D) Control and VDR-4 shRNA cells were treated with $1,25(OH)_2D_3$ or vehicle for 1 h and RhoA activity was determined by GST pulldown. Normalized RhoAGTP levels are expressed as the mean ± SD (n = 3). (E) Control and VDR-4 shRNA cells were treated with $1,25(OH)_2D_3$ or vehicle for 2 h and the level of phospho- and total p38MAPK was determined by WB (mean ± SD, n = 3). (F) Control and VDR-4 shRNA cells were treated with $1,25(OH)_2D_3$ or vehicle for 2 h and the level of phospho-MSK1 (p-MSK1) and phospho-CREB (p-CREB) in nuclear (N) and cytosolic (C) fractions was determined by WB. Total CREB and lamin B and β-tubulin were used as respective controls. *, $P < 0.05$; ***, $P < 0.001$.

OPN RNA in IMR90, HaCaT, and NIH 3T3 cells, that of *CYP3A* RNA in IMR90 and HaCaT cells, and that of *CYP24* RNA in human Caco-2 colon and MCF-7 breast cancer cells (Fig. S5).

The activation of p38MAPK-MSK1 is a downstream RhoA-ROCK event that is necessary for the interference of the Wnt–β-catenin pathway by $1,25(OH)_2D_3$

Ro318220 did not prevent the rise in $[Ca^{2+}]_{cyt}$, indicating that Ca^{2+} influx is independent of MSK1 activation (Fig. 9 A). Likewise, Ro318220 neither inhibited the increase in the level of RhoAGTP (unpublished data) or of phosphorylated cofilin by $1,25(OH)_2D_3$ nor affected phospho-PRK2 (Fig. S4). The activation of p38MAPK and MSK1 by $1,25(OH)_2D_3$ was absent in N19-RhoA cells (Fig. 9 B). In line with this, the level of phosphorylated CREB and ATF1 was increased by $1,25(OH)_2D_3$ in mock cells but did not change in N19-RhoA cells (Fig. 9 B). Concordantly, pretreatment with Y27632 inhibited the increase of phosphorylated p38MAPK, MSK1, CREB, and ATF1 by $1,25(OH)_2D_3$ in SW480-ADH cells (unpublished data). In addition, SB203580 or Ro318220 further reduced the induction of E-cadherin and *CYP24* RNA by $1,25(OH)_2D_3$ in N19-RhoA cells (Fig. 9, C and D). Collectively, these results indicate that the p38MAPK-MSK1 module acts downstream of RhoA.

Finally, Ro318220 prevented the inhibition of the transcriptional activity of β-catenin–TCF complexes by $1,25(OH)_2D_3$ (Fig. 9 E). This indicates that MSK1 also mediates the antagonism of the Wnt–β-catenin pathway by $1,25(OH)_2D_3$.

Discussion

Natural and synthetic vitamin D compounds are increasingly studied as anticancer agents (Deeb et al., 2007). Our results highlight a signaling pathway triggered by $1,25(OH)_2D_3$ that starts with the Ca^{2+} influx from the external medium and continues with the activation of RhoA–ROCK and then of the p38MAPK-MSK1 kinase module. These are necessary steps for the regulation of gene expression, the antagonism of the Wnt–β-catenin pathway, and the induction of an adhesive epithelial phenotype (Fig. 9 F). The Ca^{2+} influx–RhoA–ROCK–p38MAPK-MSK1 pathway shown here links the nongenomic and genomic $1,25(OH)_2D_3$ effects and demonstrates that the rapid modulation of ion content and cytosolic GTPases and kinases is required for the regulation of gene expression and cell physiology.

The activation of the nongenomic pathway requires VDR as shown by the generation and study of VDR shRNA cells and the analysis of VDR-deficient SW480-R cells. How these rapid and transcription-independent events are triggered is unclear, as we did not detect VDR at the plasma membrane and an anti-VDR antibody failed to block Ca^{2+} influx by $1,25(OH)_2D_3$. These negative results do not rule out the presence of small amounts of VDR at the plasma membrane, as occurs with estrogen or progesterone nuclear receptors (Losel et al., 2003; Norman et al., 2004). Moreover, the lack of effect on VDR knockdown by means of shRNA and in VDR-deficient SW480-R cells is consistent with the requirement of functional VDR in osteoblasts for the modulation of ion channel responses (Zanello and Norman, 2004).

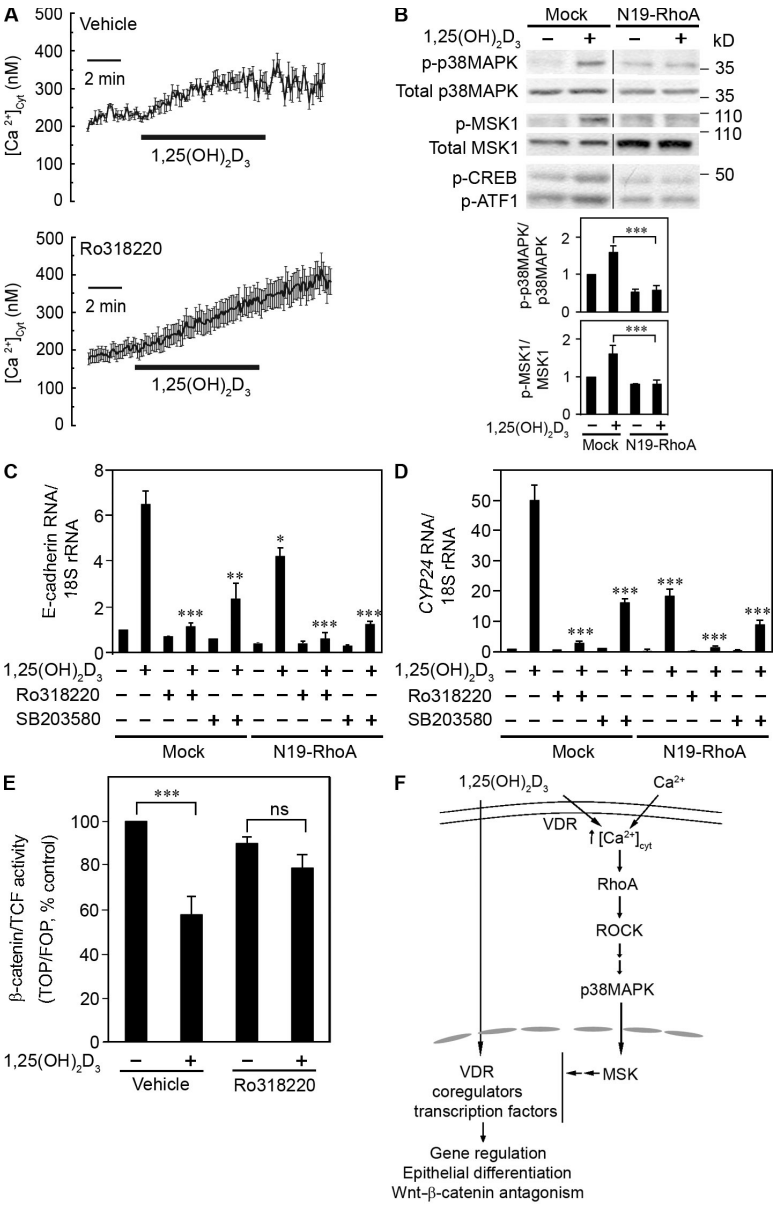

Figure 9. **p38MAPK-MSK1 activation by $1,25(OH)_2D_3$ depends on RhoA–ROCK and is necessary for the interference of the Wnt–β-catenin pathway.** (A) SW480-ADH cells were incubated with $1,25(OH)_2D_3$ in the presence of 2 μM Ro318220 or vehicle. The $[Ca^{2+}]_{cyt}$ was determined after $1,25(OH)_2D_3$ addition. Mean ± SEM of 28–30 cells (three independent experiments). (B) Mock and N19-RhoA cells were incubated with $1,25(OH)_2D_3$ or vehicle (2 h) and the levels of total and phospho-p38MAPK, -MSK1, -CREB, and -ATF1 were determined by WB. Mean ± SD (n = 3). (C) Mock and N19-RhoA cells were pretreated with vehicle, 30 μM Ro318220, or 30 μM SB203580 (2 h) and then incubated with $1,25(OH)_2D_3$ for additional 4 h, and the level of E-cadherin RNA was determined by qRT-PCR. Mean ± SD (three independent experiments performed in triplicate). (D) Mock and N19-RhoA cells were incubated (4 h) with $1,25(OH)_2D_3$ in the presence of vehicle, Ro318220, or SB203580, and the level of *CYP24* RNA and quantification was determined as in C. (E) SW480-ADH cells were transfected with wild-type (TOP) or mutant (FOP) reporter plasmids for β-catenin–TCF activity. After overnight incubation, the cells were treated (48 h) with either vehicle or $1,25(OH)_2D_3$ in the presence or absence of 1 μM Ro318220. Mean ± SD (n = 3). (F) Scheme of the mechanism of action of $1,25(OH)_2D_3$ in human SW480-ADH cells. A rapid, VDR-dependent nongenomic signaling pathway that starts with Ca^{2+} influx and continues with the sequential activation of RhoA GTPase and the kinases ROCK, p38MAPK, and MSK1 converges in the nucleus with ligand-activated VDR to regulate gene expression and interfere with the Wnt–β-catenin pathway leading to proliferation arrest and epithelial differentiation. MSK1 may target VDR and/or its coregulators and/or downstream transcription factors. *, P < 0.05; **, P < 0.01; ***, P < 0.001.

VDR may not be the only receptor for $1,25(OH)_2D_3$ (Nemere et al., 2004). However, the evidence from studies using cultured cells and genetically modified mice suggests that most $1,25(OH)_2D_3$ actions are mediated by VDR (Erben et al., 2002). We conclude that the initial Ca^{2+} influx is mediated by cytosolic VDR, although low membrane VDR levels as well as the binding of $1,25(OH)_2D_3$ to a Ca^{2+} channel or an associated membrane protein cannot be ruled out. The conformational change induced by ligand binding in cytosolic VDR may trigger the initial signal, perhaps indirectly by releasing putative associated factors. The cytosolic fraction of VDR has recently been localized in the vicinity of the plasma membrane in leukemia cells (Gocek et al., 2007), which would tend to support this hypothesis. Our findings imply a dual action of VDR, as a signaling molecule at the plasma membrane–cytosol and as a transcription factor within the nucleus.

The use of antagonists indicates that L-type voltage-gated calcium channels mediate the Ca^{2+} influx induced by $1,25(OH)_2D_3$, as it has been recently reported in the case of the vitamin D analogue elocalcitol in human and rat bladder smooth muscle cells (Morelli et al., 2008). Interestingly, the expression of the α1c isoform of this channel is elevated in colon cancer as compared with adjacent normal mucosa (Wang et al., 2000), which is compatible with an effect of $1,25(OH)_2D_3$ in this neoplasia.

The role of RhoA in the induction of *CDH1*/E-cadherin and other target genes and the profound phenotypic change induced by $1,25(OH)_2D_3$ are consistent with its key function regulating the cytoskeleton, endocytosis, cell polarity, migration, gene transcription, proliferation, differentiation, and oncogenesis (Burridge and Wennerberg, 2004). The inhibitory effects of N19-RhoA and Y27632 on the induction and redistribution of tight junction and adherens junction proteins by $1,25(OH)_2D_3$ indicate that RhoA activation is crucial for the acquisition of polarity and the adhesive phenotype, respectively, which are characteristics of differentiated epithelial cells. Rho GTPases and E-cadherin function control each other: stable localization of E-cadherin at the adherens junctions requires Rho activity, whereas RhoA is inhibited

by E-cadherin (Braga et al., 1997, 1999; Noren et al., 2001; Braga and Yap, 2005; Reynolds, 2007). The effect of $1,25(OH)_2D_3$ on RhoA is transient. The rapid activation of RhoA may be a response to the increase in $[Ca^{2+}]_{cyt}$, whereas the down-regulation may be a consequence of the later accumulation of E-cadherin and p120-catenin at the plasma membrane, as E-cadherin activates and p120-catenin recruits the Rho inhibitor p190RhoGAP (Noren et al., 2001, 2003; Wildenberg et al., 2006). This transient nature of RhoA activation is probably crucial, as we were unable to generate SW480-ADH cells stably expressing constitutively active RhoA caused by cytotoxicity.

MSK1, the downstream kinase activated, is predominantly nuclear, although its presence in the cytosol has also been documented, and it participates in the nucleosome response associated with immediate-early gene induction (Thomson et al., 1999). MSK1 may phosphorylate VDR and/or its coregulators or components of any of the multiprotein complexes (DRIP-TRAP and Mediator) involved in transcriptional control by $1,25(OH)_2D_3$-VDR. Perhaps a more plausible role of MSK1 may be the regulation of downstream transcription factors: MSK1 may recruit coactivators or promote interactions with chromatin-modifying or -remodeling complexes through its ability to phosphorylate transcription factors such as CREB or ATF1 or the histone H3 tail (Dunn et al., 2005). Recently, ERK activation by progestins has been reported to cause progesterone receptor phosphorylation and MSK1 activation, which is followed by recruitment of a complex of the three proteins to a nucleosome on the mouse mammary tumor virus promoter and its subsequent induction (Vicent et al., 2006). Putatively, MSK1 (and possibly the 75% homologous MSK2, according to the knockdown experiments) plays similar roles in gene activation by $1,25(OH)_2D_3$. In the case of E-cadherin it depends on p38MAPK-MSK1 activation, but in the case of *CYP24* it also depends on MKK1-ERK and PKA. Additionally, the finding that the antagonism of the Wnt–β-catenin pathway by $1,25(OH)_2D_3$, which is mediated by VDR–β-catenin interaction (Pálmer et al., 2001; Shah et al., 2006), is sensitive to Ro318220 points to effects of MSK1 at the VDR level.

Our results raise interesting questions such as the role of nuclear versus cytosolic VDR, how Ca^{2+} can activate RhoA, or which are the MSK1 substrates relevant for $1,25(OH)_2D_3$ action. These questions and whether the Ca^{2+} influx–RhoA–ROCK–p38MAPK-MSK1 pathway is responsible for or participates in $1,25(OH)_2D_3$ action in other cellular processes will require further work. The identification of this route as crucial for the control of human colon carcinoma cell proliferation and phenotype opens novel possibilities of pharmaceutical intervention for the second most lethal neoplasia worldwide (Jemal et al., 2006).

Materials and methods

Cell culture and transfections

Tumoral human SW480-ADH and SW480-R cells (derived from the SW480 cell line by limit dilution [Pálmer et al., 2001]), HT29, Caco-2 (colon) and MCF-7 (breast) cells, and nontumoral human IMR90 (fibroblasts) and HaCaT (keratinocytes), rat IEC18 (intestine), and mouse NIH 3T3 (fibroblasts) cells were cultured in DME plus 10% fetal bovine serum (Invitrogen). SW480-ADH-E-cadherin cells were previously described (Aguilera et al., 2007). All experiments using $1,25(OH)_2D_3$ (provided by R. Bouillon and A. Verstuyf, Katholieke Universiteit, Leuven, Belgium, and J.P. van de Velde, Solvay, Weesp, Netherlands) were performed in DME supplemented with charcoal-treated serum. To ensure dose dependence, $1,25(OH)_2D_3$ was used in the range 10^{-9} to 10^{-7} M; data shown correspond to 10^{-7} M unless specified (see Calcium imaging section). Cells were transfected using the jetPEI reagent (PolyPlus Transfection), achieving an efficiency of 60% as judged by fluorescence. In transient transfections, *Firefly* (Luc) and *Renilla reniformis* luciferase (Rluc) activities were measured separately using the Dual Luciferase reagent kit (Promega) and a Lumat LB9507 luminometer (Berthold). Luc activity was normalized to the Rluc activity. The human *CYP24* promoter (−367/+1 fragment containing two vitamin D response elements at −293/−273 and −172/−143 positions), luciferase reporter, and VDR expression plasmids were a gift from A. Aranda (Instituto de Investigaciones Biomédicas, Madrid, Spain); and the RhoA constructs were obtained from P. Crespo (Instituto de Biomedicina y Biotecnología de Cantabria, Santander, Spain). The *CDH1*/E-cadherin promoter activity was studied using the −987-TK-Luc construct (Pálmer et al., 2001). To study β-catenin–TCF transcriptional activity we used the TOP-Flash and FOP-Flash plasmids containing multimerized wild-type (CCTTTGATC) or mutated (CCTTTGGCC) TCF/LEF-1 binding sites upstream of a minimal *c-fos* promoter driving luciferase gene expression (Korinek et al., 1997; a gift from H. Clevers, Hubrecht Institute and University Medical Center, Utrecht, Netherlands). Mock and N19-RhoA cells were generated by stable transfection of SW480-ADH cells with HA-tagged empty vector or N19-RhoA cDNA and selection with 0.3 mg/ml G418 (Sigma-Aldrich).

Gene silencing

To knock down VDR expression, SW480-ADH cells were infected with lentiviral particles containing a U6 promoter driven by an shRNA targeting VDR. These constructs belong to the MISSION TRC-Hs 1.0 shRNA library (Sigma-Aldrich). Infected cells were selected with puromycin at 1 µg/ml. Control cells were infected with lentivirus bearing a nontargeting shRNA that activates the RISC complex and the RNA interference pathway but that contains at least five mismatched nucleotides compared with any human gene (clone SHC002; Sigma-Aldrich). MSK1 and MSK2 siRNA oligonucleotides (siGENOME SMART pool MSK1 and MSK2; Thermo Fisher Scientific) and control oligonucleotides (siControl nontargeting siRNA pool #1; Thermo Fisher Scientific) were transfected using Lipofectamine 2000 in OPTIMEM medium (both from Invitrogen). Transfection efficiency was judged to be >90% using fluorescent-labeled oligonucleotides.

Inhibitors

The inhibitor C3 exoenzyme (Rho) was obtained from Cytoskeleton, Inc.; Ro318220 (PKC, MSK, p70S6K1, PRK2, GSK-3β, and p90S6K1/RSK1), SB203580 (p38MAPK), GF109203X (PKC), Y27632 (ROCK), H89 (PKA, MSK1, and S6K1), Rp-cAMP (PKA specific), PD98059 and U0126 (MKK1), and rapamycin (mTOR-S6K1) were obtained from EMD. The potency and specificity of these kinase inhibitors have been reported elsewhere (Davies et al., 2000). The transcription inhibitors actinomycin D and DRB, the p38MAPK activator anisomycin, and lysophosphatidic acid were obtained from Sigma-Aldrich. Nimodipine and $LaCl_3$ were obtained from Bayer AG and Sigma-Aldrich, respectively.

Antibodies

We used primary mouse monoclonal antibodies against RhoA and phospho-ERK1/2 (Santa Cruz Biotechnology, Inc.); Cdc42, Rac, E-cadherin, β- and p120-catenin, PRK2, and paxillin (BD); integrin α3 (Millipore); β-tubulin (Sigma-Aldrich); $p21^{CIP1}$ (Millipore); HA (Babco); rat monoclonal antibodies against VDR (Millipore) and MSK2 (R&D Systems); rabbit polyclonal antibodies against RhoA, cyclin D1, and ERK2 (Santa Cruz Biotechnology, Inc.); α-catenin (Sigma-Aldrich); total and phosphocofilin, phospho-p38MAPK, -S6K1, -CREB (Ser^{133})/ATF1, -MSK1 (Ser^{581}), -PRK2, -histone H3 (Ser^{10}), and -PKD (Cell Signaling Technology); occludin, ZO-1, and claudin-7 (Invitrogen); and goat polyclonal antibodies against β-actin, lamin B, MSK1, and DKK-1 (Santa Cruz Biotechnology, Inc.).

RNA synthesis

30,000 cells were seeded in 24-well dishes. After overnight incubation, cells were pulsed with 1 µCi/ml [5-^{3}H]uridine 5′-triphosphate (Hartmann Analytic) for 4 h in the presence of the indicated doses of actinomycin D or vehicle (added 30 min before). At the end of the labeling period, the medium was removed and the cells were rinsed twice in PBS and fixed with chilled 10% trichloroacetic acid for 10 min. Trichloroacetic acid was then removed and the monolayers were washed in ethanol and air dried at room temperature for 20 min. Thereafter, precipitated macromolecules were dissolved in 500 µl of 0.5 N NaOH-0.1% SDS and 450 µl of each sample was diluted in 5 ml of scintillation solution OptiPhase HiSafe (PerkinElmer).

Radioactivity was measured on a 1209 RackBeta counter (LKB Wallac; PerkinElmer).

Calcium imaging

Cells were plated at ~0.5 × 10^6 cells/ml on 12-mm glass coverslips treated with poly-L-Lysine and incubated with 4 µM fura2/AM for 60 min at room temperature in external medium containing 145 mM NaCl, 5 mM KCl, 1 mM $CaCl_2$, 1 mM $MgCl_2$, 10 mM glucose, and 10 mM Hepes/NaOH, pH 7.42. For Ca^{2+}-free conditions, $CaCl_2$ was replaced by 0.5 mM EGTA. Coverslips were then placed on the heated stage (37°C) of an inverted microscope (Diaphot [Nikon]; Axiovert S100 TV [Carl Zeiss, Inc.]) and continuously perfused with prewarmed (37°C) external medium containing either vehicle or 1,25$(OH)_2D_3$. Cells were then epi-illuminated alternately at 340 and 380 nm. Light emitted above 520 nm was recorded with a Magical Image Processor (Applied Imaging) or a camera (Orca-ER ; Hamamatsu Photonics). Pixel by pixel ratios of consecutive frames were captured and $[Ca^{2+}]_{cyt}$ was estimated from these ratios as reported (Villalobos et al., 2001). 1,25$(OH)_2D_3$ was usually used at 4 × 10^{-7} M because the relative abundance of responsive cells is larger than at 10^{-7} M (see Results). The increase in $[Ca^{2+}]_{cyt}$ was however the same at both doses (compare results in Fig. 2 A and Fig. S1).

Western blotting (WB) and immunoprecipitation assays

Whole-cell extracts were prepared by washing the monolayers twice in PBS and cell lysis was done by incubation in RIPA buffer (150 mM NaCl, 1.5 mM $MgCl_2$, 10 mM NaF, 10% glycerol, 4 mM EDTA, 1% Triton X-100, 0.1% SDS, 1% deoxycholate, and 50 mM Hepes, pH 7.4) plus phosphatase- and protease-inhibitor mixture (25 mM β-glycerophosphate, 1 mM Na_3VO_4, 1 mM PMSF, 10 µg/ml leupeptin, and 10 µg/ml aprotinin) for 15 min on ice followed by centrifugation at 13,000 rpm for 10 min at 4°C. To obtain subcellular extracts the cells were washed in cold PBS and disrupted using a hypotonic lysis buffer (0.5% NP-40, 10 mM Hepes, 10 mM KCl, 0.1 mM EDTA, 0.1 mM EGTA, pH 7.9, 1 mM DDT, 1 mM PMSF, 1 mM Na_3VO_4, and 10 µg/ml aprotinin, leupeptin, and pepstatin). Lysates were centrifuged 11,000 *g* for 10 min at 4°C, and supernatants containing the cytosolic and membrane protein extract were maintained at −80°C until analysis. Pellets containing nuclei were lysed with hypertonic buffer (0.5% NP-40, 20 mM Hepes, 0.4 M NaCl, 1 mM EDTA, 1 mM EGTA, pH 7.9, 1 mM DDT, 1 mM PMSF, 1 mM Na_3VO_4, and 10 µg/ml aprotinin, leupeptin, and pepstatin) and centrifuged at 11,000 *g* at 4°C for 6 min, and supernatants were conserved at −80°C. The protein concentration was measured using the DC protein assay kit (Bio-Rad Laboratories). WB of cell lysates or immunoprecipitates was performed by electrophoresis in SDS gels and by protein transfer to Immobilon P membranes (Millipore). The membranes were incubated with the appropriate primary and secondary horseradish peroxidase–conjugated antibodies, and the antibody binding was visualized using the ECL detection system (GE Healthcare). Quantification was done by densitometry using ImageJ software.

GST pull-down assays

The activation of RhoA, Rac, and Cdc42 was assessed by affinity precipitation of the GST-bound form of these GTPases using the GST-rhotekin binding domain for RhoA and the GST-CRIB domain of PAK1 for Rac and Cdc42 as described previously (Azim et al., 2000; Ren and Schwartz, 2000). For in vivo binding assays, human cells were washed twice in ice-cold PBS and lysed, incubated with the GST fusion protein on glutathione-Sepharose beads, and analyzed as described previously (Azim et al., 2000; Ren and Schwartz, 2000). After the pulldown assay, the eluted active RhoA, Rac, or Cdc42 was detected by WB. Total protein was measured in the cell lysates that were used for the pulldown studies and served as loading controls.

Immunofluorescence and confocal microscopy

Cells were rinsed once in PBS, fixed in 3.7% paraformaldehyde for 15 min at room temperature, and rinsed once in 0.1 M glycine and twice in PBS. The cells were permeabilized in 0.5% Triton X-100 and then washed three times in PBS. Nonspecific sites were blocked by incubation with PBS containing 1% goat serum for 30 min at room temperature before incubating the cells with the primary antibodies diluted in PBS for 3 h at room temperature or overnight at 4°C. After four washes in PBS, the cells were incubated with secondary antibodies for 45 min at room temperature, washed three times in PBS, and mounted in VectaShield (Vector Laboratories). F-actin was stained with Texas red–labeled phalloidin (Sigma-Aldrich) for 10 min at room temperature followed by four washes in PBS. The secondary antibodies used include the following: FITC-conjugated goat anti–mouse IgG (Jackson ImmunoResearch Laboratories) and FITC-conjugated goat anti–rabbit IgG (heavy light chains; Vector Laboratories). Images of immunolabeled samples were obtained at 20°C with a laser-scanning confocal microscope (LSM 510; Carl Zeiss, Inc.) using plan apochromat immersion oil 63x NA 1.4 objective lens and argon ion (488 nm) and HeNe (543 nm) lasers. Images were acquired sequentially by direct register using LSM software (Carl Zeiss, Inc.) without manipulation; for double labeling experiments, images of the same confocal plane were generated and superimposed. Phase-contrast images were captured with a digital camera (DC300; Leica) mounted on an inverted microscope (Labovert FS; Leitz). TIFF images were processed using Photoshop 7.0 software (Adobe).

Quantitative RT-PCR (qRT-PCR)

Total RNA was purified using RNeasy mini kits following the manufacturer's instructions (QIAGEN). To measure the RNA levels for *CDH1*/E-cadherin, *OPN*, *OCN*, *CYP3A*, and *GAPDH*, we used oligonucleotides (5′-AGAACGCATTGCCACATACACTC-3′ and 5′-CATTCTGATCGGTTACCGTGATC-3′ for *CDH1*/E-cadherin; 5′-TTGCAGTGATTTGCTTTTGC-3′ and 5′-GTCATGGCTTTCGTTGGACT-3′ for *OPN*; 5′-GCACAGCCCAGAGGGTATAA-3′ and 5′-CGCCTGGGTCTCTTCACTAC-3′ for *OCN*; 5′-GATGAAAGAAAGTCGCCTCG-3′ and 5′-TGCAGTTTCTGCTGGACATC-3′ for *CYP3A*; 5′-ACAGTCCATGCCATCACTGCC-3′ and 5′-CTAGCTGACCTCCTTGACCTG-3′ for *GAPDH*) and SYBR green, and for *CYP24* and *18S* rRNA, we used TaqMan probes (Applied Biosystems) with a 7900HT fast real-time PCR system (Applied Biosystems). The PCR cycling conditions used were as follows: incubation at 95°C for 10 min followed by 40 cycles of 15 s at 95°C, 60 s at 60°C, and 5 s at 72°C. At the end of the PCR cycles, melting curve analyses were performed, and the extent of induction was calculated as described previously (Perakyla et al., 2005).

Statistical analysis

The data are expressed as the mean ± SD unless otherwise specified. Statistical significance was assessed by two-tailed unpaired student's *t* test. The single asterisk indicates $P < 0.05$, the double asterisk $P < 0.01$, and the triple asterisk $P < 0.001$. When $P > 0.05$, the data were considered not significant. All statistical analyses were performed using Instat 3.0 software (GraphPad).

Online supplemental material

Fig. S1 shows controls for transcription inhibition by actinomycin D and DRB in SW480-ADH cells and the specificity of the increase of $[Ca^{2+}]_{cyt}$ by 10^{-7} M 1,25$(OH)_2D_3$. Fig. S2 shows the lack of effect of N19-RhoA on VDR expression in SW480-ADH cells and of C3 exoenzyme and Y27632 on E-cadherin expression in SW480-ADH-E-cadherin cells and the dependence on RhoA–ROCK of the induction of claudin-7 and occludin by 1,25$(OH)_2D_3$. Fig. S3 shows the inhibition by N19-RhoA and Y27632 of the induction of paxillin, stress fibers, and focal contacts by 1,25$(OH)_2D_3$. Fig. S4 shows a scheme of the action of the kinase inhibitors used, their effect on cell viability, on E-cadherin expression and S6K1 phosphorylation (rapamycin), on histone H3 (GF109203X, Ro318220, SB203580, H89, and Rp-cAMP), on MSK (H89, Ro318220, and SB203580), and on cofilin and PRK2 phosphorylation (Ro318220). Additionally, it shows the effect of PD98059 on *CYP24* promoter activation induced by 1,25$(OH)_2D_3$. Fig. S5 shows the inhibitory effect of Ro318220 and SB203580 on the induction of CREB phosphorylation, the activation of *CYP24*, *OPN*, and *CYP3A* promoters, and the increase of *CYP24* RNA levels by 1,25$(OH)_2D_3$ in a panel of normal and tumoral cell lines of human and rodent origin. Online supplemental material is available at http://www.jcb.org/cgi/content/full/jcb.200803020/DC1.

We are grateful to those who provided us with materials and to T. Iglesias and L. González-Santiago for advice with the kinase and immunoprecipitation studies. We also thank D. Navarro and T. Martínez for their technical assistance and R. Rycroft for his help with the English manuscript.

This work was supported by the Ministerio de Ciencia e Innovación (SAF2007-60341), the Ministerio de Sanidad y Consumo (Instituto de Salud Carlos III-Redes Temáticas de Investigación Cooperativa; RD06/0020/0009), the Comunidad de Madrid (S-GEN-0266/2006), and the European Union (MRTN-CT-2005-019496; NucSys).

Submitted: 4 March 2008
Accepted: 20 October 2008

References

Agoston, E.S., M.A. Hatcher, T.W. Kensler, and G.H. Posner. 2006. Vitamin D analogs as anti-carcinogenic agents. *Anticancer Agents Med. Chem.* 6:53–71.

Aguilera, O., C. Peña, J.M. García, M.J. Larriba, P. Ordóñez-Morán, D. Navarro, A. Barbáchano, I.L. de Silanes, E. Ballestar, M.F. Fraga, et al. 2007.

The Wnt antagonist *DICKKOPF-1* gene is induced by 1α,25-dihydroxyvitamin D_3 associated to the differentiation of human colon cancer cells. *Carcinogenesis.* 28:1877–1884.

Azim, A.C., K.L. Barkalow, and J.H. Hartwig. 2000. Determination of GTP loading on Rac and Cdc42 in platelets and fibroblasts. *Methods Enzymol.* 325:257–263.

Braga, V.M., and A.S. Yap. 2005. The challenges of abundance: epithelial junctions and small GTPase signalling. *Curr. Opin. Cell Biol.* 17:466–474.

Braga, V.M., L.M. Machesky, A. Hall, and N.A. Hotchin. 1997. The small GTPases Rho and Rac are required for the establishment of cadherin-dependent cell–cell contacts. *J. Cell Biol.* 137:1421–1431.

Braga, V.M., A. Del Maschio, L. Machesky, and E. Dejana. 1999. Regulation of cadherin function by Rho and Rac: modulation by junction maturation and cellular context. *Mol. Biol. Cell.* 10:9–22.

Burridge, K., and K. Wennerberg. 2004. Rho and Rac take center stage. *Cell.* 116:167–179.

Campbell, M.J., and L. Adorini. 2006. The vitamin D receptor as a therapeutic target. *Expert Opin. Ther. Targets.* 10:735–748.

Davies, S.P., H. Reddy, M. Caivano, and P. Cohen. 2000. Specificity and mechanism of action of some commonly used protein kinase inhibitors. *Biochem. J.* 351:95–105.

Deak, M., A.D. Clifton, L.M. Lucocq, and D.R. Alessi. 1998. Mitogen- and stress-activated protein kinase-1 (MSK1) is directly activated by MAPK and SAPK2/p38, and may mediate activation of CREB. *EMBO J.* 17:4426–4441.

Deeb, K.K., D.L. Trump, and C.S. Johnson. 2007. Vitamin D signalling pathways in cancer: potential for anticancer therapeutics. *Nat. Rev. Cancer.* 7:684–700.

Dunn, K.L., P.S. Espino, B. Drobic, S. He, and J.R. Davie. 2005. The Ras-MAPK signal transduction pathway, cancer and chromatin remodeling. *Biochem. Cell Biol.* 83:1–14.

Erben, R.G., D.W. Soegiarto, K. Weber, U. Zeitz, M. Lieberherr, R. Gniadecki, G. Moller, J. Adamski, and R. Balling. 2002. Deletion of deoxyribonucleic acid binding domain of the vitamin D receptor abrogates genomic and nongenomic functions of vitamin D. *Mol. Endocrinol.* 16:1524–1537.

Giovannucci, E., Y. Liu, E.B. Rimm, B.W. Hollis, C.S. Fuchs, M.J. Stampfer, and W.C. Willett. 2006. Prospective study of predictors of vitamin D status and cancer incidence and mortality in men. *J. Natl. Cancer Inst.* 98:451–459.

Glotzer, M. 2005. The molecular requirements for cytokinesis. *Science.* 307:1735–1739.

Gocek, E., M. Kielbinski, and E. Marcinkowska. 2007. Activation of intracellular signaling pathways is necessary for an increase in VDR expression and its nuclear translocation. *FEBS Lett.* 581:1751–1757.

Grant, W.B., and C.F. Garland. 2004. A critical review of studies on vitamin D in relation to colorectal cancer. *Nutr. Cancer.* 48:115–123.

Huhtakangas, J.A., C.J. Olivera, J.E. Bishop, L.P. Zanello, and A.W. Norman. 2004. The vitamin D receptor is present in caveolae-enriched plasma membranes and binds 1α,25$(OH)_2$-vitamin D_3 in vivo and in vitro. *Mol. Endocrinol.* 18:2660–2671.

Jemal, A., R. Siegel, E. Ward, T. Murray, J. Xu, C. Smigal, and M.J. Thun. 2006. Cancer statistics, 2006. *CA Cancer J. Clin.* 56:106–130.

Korinek, V., N. Barker, P.J. Morin, D. van Wichen, R. de Weger, K.W. Kinzler, B. Vogelstein, and H. Clevers. 1997. Constitutive transcriptional activation by β-catenin-Tcf complex in $APC^{-/-}$ colon carcinoma. *Science.* 275: 1784–1787.

Larriba, M.J., N. Valle, H.G. Pálmer, P. Ordóñez-Morán, S. Alvarez-Díaz, K.F. Becker, C. Gamallo, A.G. de Herreros, J.M. González-Sancho, and A. Muñoz. 2007. The inhibition of Wnt/β-catenin signalling by 1α,25-dihydroxyvitamin D_3 is abrogated by Snail1 in human colon cancer cells. *Endocr. Relat. Cancer.* 14:141–151.

Losel, R., and M. Wehling. 2003. Nongenomic actions of steroid hormones. *Nat. Rev. Mol. Cell Biol.* 4:46–56.

Losel, R.M., E. Falkenstein, M. Feuring, A. Schultz, H.C. Tillmann, K. Rossol-Haseroth, and M. Wehling. 2003. Nongenomic steroid action: controversies, questions, and answers. *Physiol. Rev.* 83:965–1016.

Maekawa, M., T. Ishizaki, S. Boku, N. Watanabe, A. Fujita, A. Iwamatsu, T. Obinata, K. Ohashi, K. Mizuno, and S. Narumiya. 1999. Signaling from Rho to the actin cytoskeleton through protein kinases ROCK and LIM-kinase. *Science.* 285:895–898.

Morelli, A., R. Squecco, P. Failli, S. Filippi, L. Vignozzi, A.K. Chavalmane, B. Fibbi, R. Mancina, G. Luciani, M. Gacci, et al. 2008. The vitamin D receptor agonist elocalcitol upregulates L-type calcium channel activity in human and rat bladder. *Am. J. Physiol. Cell Physiol.* 294:C1206–C1214.

Nemere, I., S.E. Safford, B. Rohe, M.M. DeSouza, and M.C. Farach-Carson. 2004. Identification and characterization of 1,25D_3-membrane-associated rapid response, steroid (1,25D3-MARRS) binding protein. *J. Steroid Biochem. Mol. Biol.* 89-90:281–285.

Noren, N.K., C.M. Niessen, B.M. Gumbiner, and K. Burridge. 2001. Cadherin engagement regulates Rho family GTPases. *J. Biol. Chem.* 276:33305–33308.

Noren, N.K., W.T. Arthur, and K. Burridge. 2003. Cadherin engagement inhibits RhoA via p190RhoGAP. *J. Biol. Chem.* 278:13615–13618.

Norman, A.W., M.T. Mizwicki, and D.P. Norman. 2004. Steroid-hormone rapid actions, membrane receptors and a conformational ensemble model. *Nat. Rev. Drug Discov.* 3:27–41.

Ordóñez-Morán, P., M.J. Larriba, N. Pendás-Franco, O. Aguilera, J.M. González-Sancho, and A. Muñoz. 2005. Vitamin D and cancer: an update of in vitro and in vivo data. *Front. Biosci.* 10:2723–2749.

Pálmer, H.G., J.M. González-Sancho, J. Espada, M.T. Berciano, I. Puig, J. Baulida, M. Quintanilla, A. Cano, A.G. de Herreros, M. Lafarga, and A. Muñoz. 2001. Vitamin D_3 promotes the differentiation of colon carcinoma cells by the induction of E-cadherin and the inhibition of β-catenin signaling. *J. Cell Biol.* 154:369–387.

Pálmer, H.G., M. Sanchez-Carbayo, P. Ordóñez-Morán, M.J. Larriba, C. Cordon-Cardo, and A. Muñoz. 2003. Genetic signatures of differentiation induced by 1α,25-dihydroxyvitamin D_3 in human colon cancer cells. *Cancer Res.* 63:7799–7806.

Perakyla, M., M. Malinen, K.H. Herzig, and C. Carlberg. 2005. Gene regulatory potential of nonsteroidal vitamin D receptor ligands. *Mol. Endocrinol.* 19:2060–2073.

Pérez-Moreno, M., C. Jamora, and E. Fuchs. 2003. Sticky business: orchestrating cellular signals at adherens junctions. *Cell.* 112:535–548.

Ren, X.D., and M.A. Schwartz. 2000. Determination of GTP loading on Rho. *Methods Enzymol.* 325:264–272.

Reynolds, A.B. 2007. p120-catenin: Past and present. *Biochim. Biophys. Acta.* 1773:2–7.

Sakurada, S., N. Takuwa, N. Sugimoto, Y. Wang, M. Seto, Y. Sasaki, and Y. Takuwa. 2003. Ca^{2+}-dependent activation of Rho and Rho kinase in membrane depolarization-induced and receptor stimulation-induced vascular smooth muscle contraction. *Circ. Res.* 93:548–556.

Sancho, E., E. Batlle, and H. Clevers. 2004. Signaling pathways in intestinal development and cancer. *Annu. Rev. Cell Dev. Biol.* 20:695–723.

Schwartz, G.G., M.C. Hall, D. Stindt, S. Patton, J. Lovato, and F.M. Torti. 2005. Phase I/II study of 19-nor-1α-25-dihydroxyvitamin D_2 (paricalcitol) in advanced, androgen-insensitive prostate cancer. *Clin. Cancer Res.* 11:8680–8685.

Shah, S., M.N. Islam, S. Dakshanamurthy, I. Rizvi, M. Rao, R. Herrell, G. Zinser, M. Valrance, A. Aranda, D. Moras, et al. 2006. The molecular basis of vitamin D receptor and β-catenin crossregulation. *Mol. Cell.* 21:799–809.

Sutton, A.L., and P.N. MacDonald. 2003. Vitamin D: more than a "bone-a-fide" hormone. *Mol. Endocrinol.* 17:777–791.

Takeichi, M. 1993. Cadherins in cancer: implications for invasion and metastasis. *Curr. Opin. Cell Biol.* 5:806–811.

Thomson, S., A.L. Clayton, C.A. Hazzalin, S. Rose, M.J. Barratt, and L.C. Mahadevan. 1999. The nucleosomal response associated with immediate-early gene induction is mediated via alternative MAP kinase cascades: MSK1 as a potential histone H3/HMG-14 kinase. *EMBO J.* 18:4779–4793.

Vaisanen, S., T.W. Dunlop, L. Sinkkonen, C. Frank, and C. Carlberg. 2005. Spatio-temporal activation of chromatin on the human CYP24 gene promoter in the presence of 1α,25-Dihydroxyvitamin D3. *J. Mol. Biol.* 350:65–77.

van de Wetering, M., E. Sancho, C. Verweij, W. de Lau, I. Oving, A. Hurlstone, K. van der Horn, E. Batlle, D. Coudreuse, A.P. Haramis, et al. 2002. The β-catenin/TCF-4 complex imposes a crypt progenitor phenotype on colorectal cancer cells. *Cell.* 111:241–250.

Vicent, G.P., C. Ballare, A.S. Nacht, J. Clausell, A. Subtil-Rodriguez, I. Quiles, A. Jordan, and M. Beato. 2006. Induction of progesterone target genes requires activation of Erk and Msk kinases and phosphorylation of histone H3. *Mol. Cell.* 24:367–381.

Villalobos, C., L. Nunez, P. Chamero, M.T. Alonso, and J. Garcia-Sancho. 2001. Mitochondrial Ca^{2+} oscillations driven by local high Ca^{2+} domains generated by spontaneous electric activity. *J. Biol. Chem.* 276:40293–40297.

Wang, X.T., Y. Nagaba, H.S. Cross, F. Wrba, L. Zhang, and S.E. Guggino. 2000. The mRNA of L-type calcium channel elevated in colon cancer: protein distribution in normal and cancerous colon. *Am. J. Pathol.* 157:1549–1562.

Wiese, R.J., A. Uhland-Smith, T.K. Ross, J.M. Prahl, and H.F. DeLuca. 1992. Up-regulation of the vitamin D receptor in response to 1,25-dihydroxyvitamin D_3 results from ligand-induced stabilization. *J. Biol. Chem.* 267:20082–20086.

Wildenberg, G.A., M.R. Dohn, R.H. Carnahan, M.A. Davis, N.A. Lobdell, J. Settleman, and A.B. Reynolds. 2006. p120-catenin and p190RhoGAP regulate cell-cell adhesion by coordinating antagonism between Rac and Rho. *Cell.* 127:1027–1039.

Wu, K., D. Feskanich, C.S. Fuchs, W.C. Willett, B.W. Hollis, and E.L. Giovannucci. 2007. A nested case-control study of plasma 25-hydroxy-vitamin D concentrations and risk of colorectal cancer. *J. Natl. Cancer Inst.* 99:1120–1129.

Zanello, L.P., and A.W. Norman. 2004. Rapid modulation of osteoblast ion channel responses by 1α,25$(OH)_2$-vitamin D_3 requires the presence of a functional vitamin D nuclear receptor. *Proc. Natl. Acad. Sci. USA.* 101:1589–1594.